THE NEW KEYNESIAN CLIMATE MODEL

JEAN-GUILLAUME SAHUC FRANK SMETS GAUTHIER VERMANDEL

ABSTRACT. Climate change confronts economies with two inflationary challenges: *climateflation*, driven by physical climate impacts, and *greenflation*, arising from mitigation efforts. This paper develops and estimates a nonlinear New Keynesian Climate model that merges the long-term dynamics of Integrated Assessment Models with the business cycle fluctuations captured by DSGE frameworks. This unified framework enables a systematic analysis of how climate change and mitigation policies influence inflation, output, and interest rates. We find that nominal rigidities are crucial for determining optimal carbon pricing: neglecting them leads to miscalibrated carbon taxes, excessive inflation, and reduced consumption. Simulations also reveal that Paris-aligned mitigation paths generate higher inflation than laissez-faire approaches. Nonetheless, central banks can counter these inflationary pressures by adapting policy to a rising natural interest rate and accepting short-term GDP losses. These results highlight the need to align monetary frameworks with climate policy goals to ensure macroeconomic stability during the net-zero transition.

JEL: E32, E52, Q50, Q54.

Keywords: Climate change, inflation, monetary policy, environmental New-Keynesian model, environmental and economic trends, Bayesian estimation

J.-G. Sahuc: Banque de France, 31 rue Croix des Petits Champs, 75049 Paris, France, and University Paris-Nanterre (e-mail: jean-guillaume.sahuc@banque-france.fr). F. Smets: Bank for International Settlements, Centralbahnplatz 2, 4051 Basel, Switzerland, Ghent University and CEPR (frank.smets@ugent.be). G. Vermandel: CMAP, Ecole Polytechnique, Institut Polytechnique de Paris, Route de Saclay, Palaiseau, University Paris-Dauphine & PSL, LEDA UMR CNRS 8007, Place du Maréchal de Lattre de Tassigny, 75016 Paris, France, and Banque de France (e-mail: gauthier@vermandel.fr). We thank Nicoletta Batini, Ghassane Benmir, Marco Del Negro, Simon Dietz, Francesca Diluiso, Stephie Fried, Lars Peter Hansen, John Hassler, Fanny Henriet, Felix Kluber, Noémie Lisack, Anton Nakov, Conny Olovsson, Maria Sole Pagliari, Evi Pappa, Philipp Pfeiffer, Ricardo Reis, Fabien Tripier, Rick van der Ploeg as well as participants in several workshops and conferences for helpful comments The views expressed in this paper are those of the authors and do not necessarily reflect the views of the Banque de France, the Eurosystem, or the Bank for International Settlements. The authors declare that they have no relevant or material financial interests related to the research described in this paper.

1. Introduction

Conventional Integrated Assessment Models (IAMs), including those employed by the Intergovernmental Panel on Climate Change to evaluate specifically the long-term transition to a low-carbon economy, are formulated entirely in real terms and therefore do not capture the nominal and monetary dimensions of climate change and climate policy.[1] Yet, two inflationary forces, *climateflation*, stemming from climate-related disruptions to productivity, and *greenflation*, arising from transition policies such as carbon taxes and abatement spending, are increasingly shaping both the macroeconomic consequences and the political feasibility of the net-zero transition. The New-Keynesian (NK) framework, which explicitly models nominal rigidities and the transmission of monetary policy, offers a natural foundation for incorporating nominal effects. However, standard NK models are designed for short- to medium-term analysis and therefore do not capture the long-term structural transformations that characterize climate dynamics. Bridging these two perspectives calls for a unified framework that combines the long-run evolution of climate change with the nominal frictions central to monetary policy.

This paper presents the New Keynesian Climate (NKC) model, a tractable, nonlinear framework for the global economy that bridges the gap between Integrated Assessment Models and recent New Keynesian models. This new framework is deliberately designed to preserve the analytical clarity and tractability of traditional macroeconomic models, such as those of Woodford (2003) and Galí (2008), while incorporating key features to *(i)* capture climate externalities and abatement costs and *(ii)* attenuate the excessive expectation-driven effects of distant policy announcements.[2] In addition, it captures the first-order real and nominal effects of the green transition and enables a systematic analysis of the evolving role of central banks in managing its macroeconomic consequences amid long-term structural shifts.

The NKC consists of four core equations: *a discounted IS curve*, which incorporates green investment to reduce carbon emissions and applies extra discounting to future terms to reflect the weaker sensitivity of households to climate policy news; *a discounted Phillips curve*,

[1] Fernández-Villaverde et al. (2025) provide a comprehensive review of recent advances in structural IAMs, focusing on the integration of natural science with general equilibrium macroeconomic frameworks and computational methods.

[2] Under the usual assumption of rational expectations, current output and inflation respond disproportionately to announced future events through the expectations channel (Del Negro et al., 2023), a feature often referred to as the forward guidance puzzle in New Keynesian economics. This issue is not confined to monetary economics: climate-economic models are equally susceptible to overstating the short-run effects of mitigation policies and climate damages that occur far in the future. To generate empirically plausible dynamics, it is therefore necessary to dampen these expectation-driven responses, drawing on insights from the literature on Euler discounting (McKay et al., 2016; Woodford, 2019; Gabaix, 2020).

which accounts for the economic damage from rising carbon stocks and the production costs of abatement efforts, and downweights the influence of distant future inflation expectations; the monetary policy rule, which links the nominal interest rate to inflation deviations from target and the output gap; and *cumulative carbon emissions*, defined as the stock of past emissions net of abatement, which drive climate change. Importantly, the model incorporates five exogenous trends (population, carbon intensity, abatement efficiency, the inflation target, and technological progress) to account for observed structural changes over the long run. These trends are essential in macro-climate models as they enable accurate forecasts of future carbon emissions and hence climate change. Neglecting these structural trends may result in inaccurate quantitative predictions, especially concerning future climate change, which can shape expectations and, in turn, bias even current policy recommendations. Since climate change is global in nature, a tractable global economy framework is a natural starting point before turning to more disaggregated analysis. This choice also offers three main advantages: *(i)* it enables a clear analytical decomposition of inflationary effects; *(ii)* it allows for direct comparison with existing IAMs, many of which are formulated at the global level; and *(iii)* it sidesteps the complexity of modeling emissions trajectories across multiple economies. While monetary frameworks vary across countries, most central banks operate under inflation-targeting regimes and respond to shared structural forces, resulting in a strong co-movement of policy rates. In particular, the usual targets are highly correlated due to factors such as synchronized business cycles (Rey, 2015) and the globalization of supply chains, which has contributed to the emergence of a global Phillips curve (Auer et al., 2017). In this context, the NKC model offers a tractable yet reasonable representation of the aggregate interactions between climate policy and monetary policy in the face of rising temperatures or coordinated carbon taxation.

A central contribution of this paper is the full-information estimation of the NKC model using novel methods tailored to its intrinsically nonlinear structure. Whereas traditional IAMs often rely on calibration, limiting empirical validation and weakening their policy relevance (Pindyck, 2013), we introduce empirical discipline into a climate-integrated macroeconomic framework, consistent with the standards of modern quantitative macroeconomics. Persistent structural trends make conventional perturbation techniques unsuitable, as local approximations around a deterministic steady state break down. To address this, we simulate and estimate the model using unanticipated shocks (commonly referred to as "MIT shocks") and assume no aggregate uncertainty. Specifically, we develop a new filtering approach that treats the model itself as the data-generating process, enabling direct statistical evaluation against four global macroeconomic and climate-related time series from 1985Q1 to 2023Q2. Finally,

our Bayesian framework allows us to quantify parametric uncertainty across climate policy scenarios, complementing existing studies that emphasize uncertainty in emissions pathways (IPCC, 2021), long-run climate-economic risks (Cai and Lontzek, 2019; van den Bremer and van der Ploeg, 2021), and structural uncertainty in climate system calibration, which shapes the social planner's problem (Folini et al., 2025).

Armed with this estimated model, we assess the role of price rigidities and monetary policy during the green transition, specifically its response to climateflation and greenflation, across different transition scenarios. The first scenario is a "laissez-faire" economy characterized by an increasing stock of carbon, that warms the planet and making resources scarcer. The increasing damage to total factor productivity acts as a permanent negative supply shock that fuels inflation and drives output below its technological trend (Schnabel, 2022). The second scenario reflects the Paris Agreement, under which governments worldwide coordinate mitigation policies aimed at achieving net-zero carbon emissions by 2050. In our framework, this scenario takes the form of a linear increase in the carbon tax such that full abatement is reached in 2050. The rise in carbon tax forces firms to internalize the effects of their carbon emissions on aggregate productivity. In response, they reduce their emissions by increasing abatement expenditures, creating a demand-driven boom. These scenarios serve to *(i)* explore the trade-offs between immediate abatement efforts and future climate-induced damages, and *(ii)* examine their implications for natural output, natural interest rate, inflation dynamics, and the appropriate monetary policy responses.

Our analysis yields five key findings, each with important policy implications.

(1) We show that the *social cost of carbon is lower in an economy with sticky prices* than in a flexible-price setting.[3] This reflects a fundamental trade-off between price stability and climate ambition. If inflation is not well-managed during the green transition, the rising welfare cost of inflation weakens the case for aggressive carbon pricing, thereby reducing the optimal social cost of carbon. In effect, when the transition leads to sustained inflation above target, optimal climate policy becomes less ambitious: people place less value on future climate benefits when their current purchasing power is eroded by inflation. This underscores how price instability can undermine long-term environmental goals.

(2) We show that neglecting inflationary pressures in climate-economic models leads to a mispricing of the carbon tax, with important macroeconomic consequences. Yet many of the models used to inform carbon tax policy, including those underlying official

[3]The social cost of carbon is the optimal price for emitting one ton of CO_2.

estimates of the optimal tax, abstract from these effects. As a result, the carbon prices they recommend may be poorly suited to real-world conditions, where prices adjust gradually. We show that *applying misaligned carbon prices can generate significant economic costs*, including lower household consumption and additional inflationary pressure. These challenges are particularly acute during the green transition, when carbon pricing is politically sensitive. Designing climate policies that are both effective and publicly acceptable therefore requires explicitly accounting for inflation and other nominal frictions that shape economic responses.

(3) We find that a *Paris-aligned green transition produces higher and more persistent inflation than a laissez-faire scenario*, as the inflationary pressures from carbon taxation outweigh the disinflationary effects from avoided climate damages. This result is robust across alternative model specifications, including wage stickiness and investment adjustment costs.

(4) Our results underscore an intertemporal trade-off for central banks: *while climate mitigation under the Paris Agreement raises short-term volatility relative to laissez-faire, it ultimately delivers greater macroeconomic stability in the long run.*

(5) We show that *conventional Taylor rules based on fixed steady-state interest rates risk persistent inflation overshooting*, by about 0.8 percentage points per year during the transition, because they fail to account for the structural rise in the natural interest rate. Climate-adaptive monetary policy rules that internalize this shift are more effective at stabilizing inflation throughout the transition.

Related Literature. Our paper contributes to the broader literature that integrates climate considerations into micro-founded structural macroeconomic models, continuing the research agenda initiated by Nordhaus (1992) and extended in Barrage and Nordhaus (2024). This literature spans multiple dimensions, including the distributional consequences of climate adaptation (Fried, 2022), the heterogeneous effects of energy and carbon price shocks (Benmir and Roman, 2022; Auclert et al., 2023; Känzig, 2023), optimal fiscal policy responses to climate change (Barrage, 2020), the role of market structure (Finkelstein Shapiro and Metcalf, 2023; Jondeau et al., 2025), comparative evaluations of environmental policy instruments (Annicchiarico and Di Dio, 2015) and the influence of uncertainty on carbon pricing strategies (Jensen and Traeger, 2014; Cai and Lontzek, 2019; van der Ploeg and Rezai, 2020; van den Bremer and van der Ploeg, 2021).[4] Our paper also contributes to an emerging strand of research,

[4] A related strand of literature examines how the direction of technological change and shifts in the energy mix influence the cost and feasibility of the transition. While this work is important for understanding long-run structural adjustments, it is less directly connected to our focus on nominal frictions and inflation dynamics.

often referred to as the greenflation literature, which quantitatively examines the inflationary consequences of the green transition. Recent studies have investigated how climate policy interacts with monetary policy in nonlinear macroeconomic settings. For instance, Nakov and Thomas (2023), using a nonlinear New Keynesian model with climate externalities, analyze how optimal monetary policy navigates the trade-off between price stability and climate goals, with the response hinging on the optimality of climate policy itself. Other work shows that the inflationary effects of the green transition depend critically on monetary policy design and production structure. Similarly, Olovsson and Vestin (2023) and Del Negro et al. (2023) use multi-sector models with nominal rigidities to explore how sectoral substitution influences the inflationary effects of the green transition. Targeting core inflation helps contain volatility from energy price spikes, while production network complementarities amplify input cost shocks, intensifying inflation. In a small open economy setting, Pappa et al. (2023) highlight the importance of energy efficiency and the need for complementary fiscal measures to facilitate a smoother transition. Finally, Fornaro et al. (2025) show that capping dirty goods production raises inflation and steepens the Phillips curve, complicating central banks' efforts to balance inflation and output.

Our approach departs from the existing literature in several important respects, offering a distinct contribution to the analysis of the nominal consequences of climate change. First, we contribute to the greenflation literature by developing a deliberately simple framework that isolates the core inflationary mechanisms triggered by both climate policy and climate damages. While much of the literature focuses narrowly on greenflation, we extend the analysis to include climateflation. Crucially, we decompose these forces prior to general equilibrium adjustments, providing transparent accounting of their respective contributions. Although both channels are quantitatively significant ex ante, their inflationary impact may be attenuated by general equilibrium forces, particularly through wage responses. Second, unlike most existing work that relies on calibrated models, we estimate a nonlinear structural framework. This grounds our analysis in the empirical methodology of modern quantitative macroeconomics, following the tradition of Smets and Wouters (2007). As a result, our simulations are not merely illustrative: they are generated from a fully estimated model and constitute true out-of-sample forecasts. This estimation approach disciplines both the model's parameters and its initial conditions, providing a consistent basis for the transition dynamics. Third, our framework allows for full transition paths to net-zero emissions, in line with scenarios assessed by the IPCC. Much of the existing literature relies on constant elasticity of substitution (CES) production functions that reduce emissions through substitution between "brown"

and "green" inputs. While analytically convenient, this formulation tends to inhibit full decarbonization, as it implies sharply increasing relative prices as emissions approach zero. It also assumes fixed substitutability across time, despite growing empirical evidence that this elasticity may evolve (Jo and Miftakhova, 2024). By contrast, we adopt abatement cost curves from the DICE model (Barrage and Nordhaus, 2024), which are designed to be consistent with evidence synthesized in recent IPCC reports. This allows us to study a wide range of transition scenarios, ranging from continued warming to full decarbonization, within a tractable macro-environmental framework grounded in empirical evidence.

The remainder of this paper is organized as follows. Section 2 introduces the micro-foundations of the NKC and summarizes them into four core equations. Section 3 describes the data transformations and the prior and posterior distributions. Section 4 examines the effects of nominal rigidities on the social cost of carbon. Section 5 presents the anatomy of the green transition and analyzes how climateflation and greenflation phenomena may affect the world economy by 2100. Section 6 discusses the implications of the green transition for monetary policy. Section 7 reports additional exercises to assess the robustness of the results and Section 8 concludes.

2. The 4 equation New Keynesian climate (NKC) model

To establish a flexible framework conducive to analytical results, we incorporate climate dynamics, drawing on the integrated assessment framework of Nordhaus (1992) and the damage-cost approach of Golosov et al. (2014), into the standard three-equation New Keynesian model, as developed in Woodford (2003) and Galí (2008).

2.1. **Household sector.**

The economy consist of a time-varying mass l_t of ex-ante identical, atomistic, and infinitely lived households. This mass reflects the upward trend in population observed over the past 60 years, with l_t asymptotically converging to a long-run level $l_\infty > 0$, according to the process: $l_t = l_{t-1}\left(l_\infty / l_{t-1}\right)^{\ell_g}$, where $\ell_g \in [0,1]$ is the geometric rate of convergence to l_∞. Each household $i \in [0, l_t]$ maximizes its utility over time, which depends positively on consumption $c_{i,t}$ and negatively on labor supply $n^s_{i,t}$:

$$\mathbb{E}_t \left\{ \sum_{s=0}^{\infty} \tilde{\beta}_{t,t+s} \varepsilon_{b,t+s} \left[\frac{c_{i,t+s}^{1-\sigma_c} - 1}{1-\sigma_c} - \psi_{t+s} \frac{\left(n^s_{i,t+s}\right)^{1+\sigma_n}}{1+\sigma_n} \right] \right\}, \tag{1}$$

where $\mathbb{E}_t$ denotes the conditional expectation at time t, and $\tilde{\beta}_{t,t+s}$ is the technological-neutral discount factor.[5] The parameter $\sigma_c > 0$ represents the inverse of the intertemporal elasticity of substitution in consumption, while $\sigma_n > 0$ is the inverse of the Frisch labor supply elasticity. ψ_t is a scale variable determining hours worked in a balanced growth path, growing proportionally with the flow of consumption.[6] The preference shock $\varepsilon_{b,t}$, which captures unexpected changes in aggregate demand, follows an AR(1) process: $\varepsilon_{b,t} = (1-\rho_b) + \rho_c \varepsilon_{b,t-1} + \eta_{b,t}$, where $\eta_{b,t} \sim \mathcal{N}(0, \sigma_b^2)$.

In New Keynesian models, announced policies often lead to implausibly large effects in present value terms, as highlighted by the forward guidance puzzle discussed by Del Negro et al. (2023). These large effects arise from the expectation channel of demand: current aggregate demand depends not only on today's real interest rate but also on the entire expected future path of monetary policy, wages, productivity, and other shocks. In frameworks with perfectly forward-looking households and complete markets, this channel is extremely powerful, so that news about policies scheduled far in the future can produce disproportionately large immediate effects on output and inflation. This prediction is widely viewed as counterfactual, as empirical evidence suggests households are much less responsive to distant policy changes, such as mitigation policies.

To attenuate this excessive sensitivity, we follow McKay et al. (2017) and assume that households face idiosyncratic income risk and borrowing constraints. These frictions imply that a fraction of households are hand-to-mouth or nearly so, which leads to a discounted Euler equation.[7] Because households cannot perfectly insure against income fluctuations, they exhibit a higher marginal propensity to consume out of current income and respond less strongly to changes in expected future real interest rates. This heterogeneity dampens the expectation channel and yields more empirically plausible dynamics for the effects of anticipated policy changes. Specifically, households are endowed with stochastic idiosyncratic employment status $\varsigma_{i,t} \in \{0,1\}$, where 0 indicates low productivity (denoted "type L" worker) and 1 indicates high productivity (denoted "type H" worker). Productivity is drawn i.i.d. with probabilities $\Pr(\varsigma_{i,t} = 0) = \omega$ and $\Pr(\varsigma_{i,t} = 1) = 1 - \omega$. The real budget constraints for

[5] The presence of a permanent increase in technology affects the Euler equation, and consequently the natural real interest rate and the monetary policy rule. To keep the framework tractable, we mute the effect of technology on the long-run equilibrium rate by imposing: $\tilde{\beta}_{t,t+s} = \beta^s (z_{t+s}/z_t)^{\sigma_c}$ with $\beta \in (0,1)$. This assumption is standard in models featuring recursive utility functions such as Epstein-Zin for instance.

[6] If z_t denotes the trend in per capita consumption, $\psi_t = \psi z_t^{1-\sigma_c}$, with ψ as a scale parameter.

[7] The framework of McKay et al. (2017) can be interpreted as a tractable approximation of a richer heterogeneous-agent economy with uninsurable income risk and borrowing constraints, as in McKay et al. (2016).

each household type are:

$$c_{i,t} + b_{i,t} + T^s_{i,t} = \frac{r_{t-1}}{\pi_t} b_{i,t-1} + \Pi_{i,t} + w_t n^s_{i,t} + \frac{T^e_{i,t}}{1-\omega}, \text{ if } \varsigma_{i,t} = 1, \tag{2}$$

$$c_{i,t} + b_{i,t} = \frac{r_{t-1}}{\pi_t} b_{i,t-1} + d_{i,t}, \text{ if } \varsigma_{i,t} = 0, \tag{3}$$

where $b_{i,t}$ is the one-period riskless bond, r_t is the gross nominal interest rate, $\pi_t = p_t/p_{t-1}$ is gross inflation with p_t being the price index, $\Pi_{i,t}$ are real dividends from firm shares, w_t is the aggregate real wage, and $T^e_{i,t}$ is the lum-sum carbon tax transfer. Low-productivity households receive $d_{i,t}$ units of the consumption good as a transfer, while high-productivity households pay a tax of $T^s_{i,t} = \omega d_{i,t}/(1-\omega)$ to finance this transfer. The transfer is time-varying, increasing proportionally with productivity z_t and environmental damages (represented by $\Phi(m_t)$, defined subsequently).

The Euler equation for household i with productivity type $q \in \{H, L\}$ is:

$$\varepsilon_{b,t} c^{-\sigma_c}_{i,q,t} \geq \mathbb{E}_t \left\{ \frac{\tilde{\beta}_{t,t+1} \varepsilon_{b,t+1} r_t}{\pi_{t+1}} \left((1-\omega)\, c^{-\sigma_c}_{i,H,t+1} + \omega c^{-\sigma_c}_{i,L,t+1} \right) \right\}, \tag{4}$$

where $c_{i,H,t}$ and $c_{i,L,t}$ represent consumption of high- and low-productivity households, respectively. A higher ω lowers the share of households that satisfy the Euler condition, thereby dampening the forward-looking component of aggregate consumption.

2.2. **Business sector.** The business sector is characterized by final good producers who sell a homogeneous final good to households and the government. To produce, they purchase and package differentiated varieties produced by atomistic, infinitely lived intermediate goods firms that operate in a monopolistically competitive market. These intermediate goods firms contribute to climate change by emitting CO_2 as an unintended byproduct of their production process and are required to invest in abatement technologies to reduce these emissions.[8]

2.2.1. *Final good sector.* At every point in time t, a perfectly competitive sector produces a final good Y_t by combining a continuum of intermediate goods $y_{j,t}$, where $j \in [0, l_t]$, according to the technology $y_t = \left[l_t^{-1/\zeta} \int_0^{l_t} y_{j,t}^{\frac{\zeta-1}{\zeta}} \mathrm{d}j \right]^{\frac{\zeta}{\zeta-1}}$. The number of intermediate good firms owned

[8]Firms rely on a specialized sector, distinct from the goods market in which technology adopters operate. This abatement sector –referred to as the Environmental Goods and Services Sector in the international System of Environmental-Economic Accounting– develops technologies and solutions to mitigate or eliminate environmental harm from emissions and pollutants (Jondeau et al., 2025). This representation, inherited from the DICE model, encompasses *(i)* mitigative measures, such as carbon capture, air scrubbers, or emission filters that lessen pollution without altering the energy source, and *(ii)* preventive measures, such as systemic changes like energy substitution (e.g., transitioning to renewable energy) to curb emissions by eliminating fossil fuel dependence.

by households is equal to the population size l_t. The parameter $\zeta > 1$ measures the substitutability between differentiated intermediate goods. Final good-producing firms take both their output price, p_t, and the prices of intermediate goods, $p_{i,t}$, as given, and beyond their control. Profit maximization leads to the demand curve $y_{j,t} = l_t^{-1} \left(p_{j,t}/p_t\right)^{-\zeta} y_t$, from which we deduce the relationship between the price of the final good and the prices of intermediate goods $p_t \equiv \left[l_t^{-1} \int_0^{l_t} {p_{j,t}}^{1-\zeta} \mathrm{d}j\right]^{\frac{1}{1-\zeta}}$.

2.2.2. *Intermediate goods sector.* An intermediate good j is produced by a monopolistic firm using the following production function:

$$y_{j,t} = \Gamma_t n_{j,t}^d, \tag{5}$$

where Γ_t represents total factor productivity (TFP), which influences labor demand $n_{j,t}^d$.

The TFP is determined by two components:

$$\Gamma_t = z_t \Phi\left(m_t\right), \tag{6}$$

where z_t is the deterministic component of productivity, and $\Phi(m_t)$ is a damage function that captures the impact of climate change on the production process. The deterministic component follows the process $z_t = z_{t-1}(1 + g_{z,t})$, where $g_{z,t} = g_{z,t-1}\left(1 - \delta_z\right)$ is the productivity growth rate, and δ_z is the rate of decline in productivity. This formulation reflects that productivity growth has slowed over time by a factor δ_z, aligning with the observed deceleration in per capita economic growth over the past century.

Recent advances in climate science, particularly the TCRE (Transient Climate Response to Cumulative Carbon Emissions) framework, have established a robust linear relationship between global temperature increases and cumulative CO_2 emissions (Dietz et al., 2021). To maintain tractability while accurately capturing the climate damages central to our analysis, we adopt this cumulative emissions approach. Specifically, we model climate change through the stock of CO_2, which evolves according to:

$$m_t = m_{t-1} + \xi_m e_t, \tag{7}$$

where e_t denotes anthropogenic CO_2 emissions at time t, and $\xi_m \geq 0$ is a conversion factor from CO_2 to carbon. Climate damages are then specified as an exponential function of cumulative emissions, following Golosov et al. (2014):

$$\Phi(m_t) = \exp\left(-\gamma m_t\right), \tag{8}$$

where γ determines the sensitivity of damages to the carbon stock. This formulation closely approximates the damage functions commonly used in standard DICE models, but expresses damages directly as a function of cumulative carbon emissions rather than temperature.[9]

A firm's CO_2 emissions resulting from its production process are denoted by $e_{i,t}$. These emissions are subject to a carbon tax $\tau_{e,t}$, which aims to internalize the social cost of carbon emissions. As a result, the firm is incentivized to reduce its impact by investing in emission abatement technology. The abatement effort of the firm leads to a reduction of $\mu_{i,t}$ (in %) in its CO_2 emissions. The firm's emissions are given by:

$$e_{j,t} = \sigma_t \left(1 - \mu_{j,t}\right) y_{j,t} \varepsilon_{e,t},$$

where σ_t denotes aggregate carbon intensity in the production sector. The law of motion for σ_t is $\sigma_t = \sigma_{t-1}(1 - g_{\sigma,t})$, where $g_{\sigma,t}$ captures changes in the rate of carbon decoupling. These changes follow the process: $g_{\sigma,t} = (1 - \delta_\sigma)\, g_{\sigma,t-1}$, where $\delta_\sigma \in [0,1]$ is the rate of decline in the decoupling trend, reflecting the observed reduction in the emission-to-GDP ratio over the past 60 years. Additionally, a firm's carbon intensity can be temporarily affected by an aggregate exogenous emissions shock $\varepsilon_{e,t}$, given by: $\varepsilon_{e,t} = (1 - \rho_e) + \rho_e \varepsilon_{e,t-1} + \eta_{e,t}$, where $\eta_{e,t} \sim N(0, \sigma_e^2)$ captures cyclical fluctuations in the emissions-to-output ratio. An increase in $\varepsilon_{e,t}$ leads to a cyclical rise in carbon intensity in the production sector.

In practice, firms have three main options to reduce carbon emissions: (i) substituting carbon-intensive technologies with low-carbon technologies; (ii) investing in energy-saving technologies; or (iii) purchasing carbon sequestration. Much of the recent work on greenflation has primarily focused on substitutions.[10] To capture all three types of abatement actions, we introduce an abatement cost function from Barrage and Nordhaus (2024). Each abatement action links a marginal cost of reduction to a corresponding quantity of carbon abated. As the carbon price increases, a larger proportion of emissions is mitigated. This abatement cost function consolidates all forms of mitigation efforts into a simplified representation within a

[9] An alternative approach would model temperature as directly proportional to cumulative emissions, $\mathcal{T}_t = \xi_T m_t$, and compute damages using a quadratic damage function. This specification yields equivalent results while requiring an additional equation in the system.

[10] For instance, Olovsson and Vestin (2023); Nakov and Thomas (2023) examine the macroeconomic effects of decarbonization by modeling the substitution between two energy sources using a constant elasticity of substitution (CES) framework. Del Negro et al. (2023) extend this approach to a multisector setting using input-output linkages. While these studies provide valuable insights into mitigation via input substitution, they emphasize a single channel. In contrast, our framework, drawing from the DICE model, captures a broader range of CO_2 abatement strategies, including energy efficiency, clean technologies, and behavioral changes, through a more stylized aggregate representation as in Barrage and Nordhaus (2024), Bilal and Känzig (2025), or Jondeau et al. (2025).

one-good, one-sector economy. The cost of abatement is given by:

$$\mathcal{C}^a_{j,t} = \theta_{1,t}\mu^{\theta_2}_{j,t}y_{j,t}, \tag{9}$$

where $\theta_{1,t} = (p_b/\theta_2)(1-\delta_{pb})^{t-t_0}\sigma_t$ is the time-varying level of the abatement cost, $p_b > 0$ is a parameter determining the initial abatement costs, and $0 < \delta_{pb} < 1$ captures technological progress, which lowers the cost of abatement by a factor δ_{pb} each year. The literature on directed technological change typically endogenizes the rate of decline in green technologies, which is encapsulated in $\theta_{1,t}$. Finally, $\theta_2 > 0$ represents the curvature of the abatement cost function, which typically exhibits increasing returns in IAM literature.

Intermediate goods producers solve the typical two-stage problem. In the first stage, with the input price w_t given, firms seek to maximize their one-period profits:

$$\max_{\{y_{j,t},\mu_{j,t}\}} mc_{j,t}y_{j,t} - w_t\frac{y_{j,t}}{\Gamma_t} - \mathcal{C}^a_{j,t} - \tau_{e,t}\sigma_t\left(1-\mu_{j,t}\right)y_{j,t}\varepsilon_{e,t} \tag{10}$$

where $mc_{j,t}$ denotes the real marginal cost of producing one additional unit of output.

In the second stage, firms set their selling prices under the Rotemberg price -setting mechanism. The price adjustment cost under this framework is given by:

$$\mathcal{C}^p_{j,t} = \frac{\kappa}{2}\left(\frac{p_{j,t}}{p_{j,t-1}} - \pi^\star_t\right)^2\frac{y_t}{l_t} \tag{11}$$

where $\kappa > 0$ is the price stickiness parameter, y_t/l_t is the average market share per firm, and $\pi^\star_t$ is the gross inflation target. Following Ireland (2007), Fève et al. (2010) and Del Negro et al. (2015), this target follows a deterministic process as described by:

$$\pi^\star_t = \delta_{\pi^\star}\pi + (1-\delta_{\pi^\star})\pi^\star_{t-1}, \tag{12}$$

where $\delta_{\pi^\star}$ is the convergence rate reflecting the gradual adjustment of monetary authorities' inflation targets, and π is steady-state gross inflation. This trend mirrors the significant decline in inflation and nominal interest rates observed globally since the 1980s, which we attribute to the gradual adoption of inflation-targeting regimes by central banks, leading to a structural reduction in inflation rates.

To mitigate the expectation channel of inflation, we introduce an exogenous exit shock consistent with empirical evidence on firm survival rates (OECD, 2017). Following Bilbiie et al. (2012), we assume that each firm faces a "death" shock represented by an idiosyncratic variable $\nu_{j,t} \in \{0,1\}$, where $\nu_{j,t} = 0$ with probability ϑ (death) and $\nu_{j,t} = 1$ with probability $(1-\vartheta)$ (survival). Thus, the probability that a firm survives until period $t+s$ is given by

$\mathbb{E}_t\{\omega_{j,t+s}\} = (1-\vartheta)^s$. Consequently, the firm's optimization problem can be expressed as:

$$\max_{\{p_{j,t}\}} \mathbb{E}_t \left\{ \sum_{s=0}^{\infty} (1-\vartheta)^s \tilde{\beta}_{t,t+s} \frac{\lambda_{t+s}}{\lambda_t} \left(y_{j,t+s} \frac{p_{j,t+s}}{p_{t+s}} - \varepsilon_{p,t+s} mc_{j,t+s} y_{j,t+s} - \mathcal{C}^p_{j,t+s} \right) \right\}, \tag{13}$$

subject to the demand equation $y_{j,t} = l_t^{-1} \left(p_{j,t}/p_t\right)^{-\zeta} y_t$. λ_t denote the marginal utility of consumption of households and $\varepsilon_{p,t}$ is a cost-push shock that follows an AR(1) process: $\varepsilon_{p,t} = (1-\rho_p) + \rho_p \varepsilon_{p,t-1} + \eta_{p,t}$, where $\eta_{p,t} \sim \mathcal{N}(0, \sigma_p^2)$.

Since all intermediate goods firms face the same profit-maximizing problem, they set the same price $p_{j,t} = p_t$. In a symmetric equilibrium, where the expected survival rate from t to $t+s$ is given by $(1-\vartheta)^s$, the optimal pricing rule implies:

$$\kappa \left(\pi_t - \pi_t^\star\right) \pi_t = \kappa(1-\vartheta)\mathbb{E}_t \left\{ \tilde{\beta}_{t,t+1} \frac{\lambda_{t+1}}{\lambda_t} \frac{y_{t+1}}{y_t} \frac{l_t}{l_{t+1}} \left(\pi_{t+1} - \pi_{t+1}^\star\right) \pi_{t+1} \right\} + \zeta \varepsilon_{p,t} mc_t + (1-\zeta). \tag{14}$$

In the same spirit as our treatment of the Euler equation, the resulting Phillips curve discounts distant future marginal costs and inflation expectations by the survival probability, thereby dampening the impact of far-horizon shocks on current inflation dynamics.

2.3. **Public sector.** We apply both a unified fiscal rule and a unified monetary policy rule at the global level.[11] In particular, adopting a global monetary policy rule is a pragmatic modeling shortcut. While monetary frameworks differ across countries, most central banks today pursue inflation targeting regimes and operate in environments shaped by common global forces. Empirical evidence shows that real and financial cycles are increasingly synchronized across advanced economies (Rey, 2015), and global inflation dynamics are closely linked to oil, energy, and commodity prices, all inherently international in nature. The global dimension of supply chains and production networks further amplifies these linkages, with recent research documenting the emergence of a global Phillips curve driven by international input-output connections (Auer et al., 2017). As a result, policy rates across central banks exhibit substantial co-movement, and many economies face similar structural trends, such as declining natural interest rates and persistently low inflation. Given the global nature of climate change and its macroeconomic spillovers, using a unified monetary policy rule is a reasonable simplification. It enables us to capture key interactions between monetary policy and the green transition, while preserving the core insight that central banks' actions are shaped

[11] A multi-country coordination framework represents a natural extension of the model, enabling the analysis of additional effects arising from cross-country heterogeneity in economic structure, idiosyncratic business cycles, fiscal capacity, or exposure to climate risks. However, such an extension goes beyond the scope of our current analysis, which focuses on global aggregates to highlight the core macro-climate policy trade-offs.

not just by domestic, but also by international developments. In this context, a unified rule structure enhances the tractability and transparency of the model without losing sight of the broader global dynamics at play.

Given these considerations, it is reasonable to assume a unified global monetary policy rule. Global forces increasingly shape the two core targets of central banks,inflation and output, leading to strong co-movements in policy rates across countries. In our model, monetary policy is represented accordingly by a Taylor-type rule, where the short-term nominal interest rate is gradually adjusted in response to deviations of inflation and output from their respective targets:

$$\frac{r_t}{r} = \left(\frac{r_{t-1}}{r}\right)^{\phi_r} \left[\left(\frac{\pi_t^\star}{\pi}\right)\left(\frac{\pi_t}{\pi_t^\star}\right)^{\phi_\pi}\left(\frac{y_t}{y_t^\star}\right)^{\phi_y}\right]^{1-\phi_r} \varepsilon_{r,t}, \tag{15}$$

where r is the steady-state nominal interest rate, and $y_t^\star$ is the natural output, defined as the output that would prevail in imperfectly competitive markets but with flexible prices. The parameters ϕ_r, ϕ_π, ϕ_y capture the degree of interest-rate smoothing and the responsiveness of the policy rate to the inflation and output gaps, respectively. Finally, $\varepsilon_{r,t}$ is a monetary policy shock that follows the process: $\varepsilon_{r,t} = (1-\rho_r) + \rho_r \varepsilon_{r,t-1} + \eta_{r,t}$, with $\eta_{r,t} \sim N(0, \sigma_r^2)$.

Similarly, recent evidence suggests that fiscal policy is not purely a domestic phenomenon but exhibits a coordinated global dimension. For instance, Jiang and Richmond (2024) document the existence of a global fiscal cycle, showing that government debt issuance across major economies is highly synchronized, with the first principal component explaining over 60-70% of variation in debt growth. They find that this comovement is explained by correlated business cycles, common demand shocks for safe assets, and from strategic complementarity in debt issuance. Thus, the fiscal rule captures a stylized representation of global fiscal coordination, wherein short-term bonds are issued at the global level, and all revenues from the carbon tax are redistributed to households on a lump-sum basis:

$$\int_0^{l_t} b_{i,t}\mathrm{d}i + \tau_{e,t}\int_0^{l_t} e_{j,t}\mathrm{d}j = \frac{r_{t-1}}{\pi_t}\int_0^{l_t} b_{i,t-1}\mathrm{d}i + \int_0^{l_t} \Pr\left(z_{i,t}=1\right) T_{i,t}^e \mathrm{d}i. \tag{16}$$

2.4. **Aggregation.** First, we aggregate consumption for the two types of households:

$$l_t c_t = \int_0^{l_t} \Pr\left(z_{i,t}=0\right) c_{L,t}\mathrm{d}i + \int_0^{l_t} \Pr\left(z_{i,t}=1\right) c_{H,t}\mathrm{d}i, \tag{17}$$

which leads to:

$$c_t = \omega c_{L,t} + (1-\omega)\, c_{H,t}. \tag{18}$$

It is assumed that bonds are in zero net supply:

$$\int_0^{l_t} b_{i,t} \mathrm{d}i = 0. \tag{19}$$

As discussed by McKay et al. (2017), as long as $c_{L,t} < c_{H,t}$, the Euler equation for the low-productivity worker does not bind with equality, since the right-hand side will always be less than the left-hand side. Therefore, let $\lambda_t = \varepsilon_{b,t} c_{H,t}^{-\sigma_c} = \varepsilon_{b,t} \left(\frac{c_t - \omega d_t}{1-\omega} \right)^{-\sigma_c}$ denote the marginal utility of consumption of high-productivity households. The *aggregate* Euler equation is then given by:

$$\lambda_t = \mathbb{E}_t \left\{ \frac{\tilde{\beta}_{t,t+1} r_t}{\pi_{t+1}} \left((1-\omega) \lambda_{t+1} + \omega \varepsilon_{b,t+1} d_{t+1}^{-\sigma_c} \right) \right\}. \tag{20}$$

In contrast, the general equilibrium condition for hours worked is:

$$(1-\omega)\, n_t^s = n_t^d. \tag{21}$$

Finally, the resource constraint is given by:

$$y_t = l_t c_t + \frac{\kappa}{2} \left(\pi_t - \pi_t^\star \right)^2 y_t + \theta_{1,t} \mu_t^{\theta_2} y_t. \tag{22}$$

2.5. **Final system.** The final system can be summarized by the following set of four core equations, which determine: *(i)* detrended GDP ($\tilde{y}_t = y_t / (l_t z_t)$), *(ii)* the nominal interest rate (r_t), *(iii)* the inflation rate (π_t), and *(iv)* the cumulative stock of carbon emissions (m_t).

(1) *Investment-Saving (IS) curve:*

$$\tilde{\lambda}_t = \beta \mathbb{E}_t \left\{ \frac{r_t}{\pi_{t+1}} \left((1-\omega)\, \tilde{\lambda}_{t+1} + \omega \varepsilon_{b,t+1} \tilde{d}_{t+1}^{-\sigma_c} \right) \right\}, \tag{23}$$

(2) *Phillips Curve (PC):*

$$\left(\pi_t - \pi_t^\star \right) \pi_t = (1-\vartheta) \beta \mathbb{E}_t \left\{ (1 + g_{z,t+1}) \frac{\tilde{\lambda}_{t+1}}{\tilde{\lambda}_t} \frac{\tilde{y}_{t+1}}{\tilde{y}_t} \left(\pi_{t+1} - \pi_{t+1}^\star \right) \pi_{t+1} \right\} + \frac{\zeta}{\kappa} \varepsilon_{p,t} m c_t + \frac{1-\zeta}{\kappa}, \tag{24}$$

(3) *Monetary Policy (MP) rule:*

$$\frac{r_t}{r} = \left(\frac{r_{t-1}}{r} \right)^{\phi_r} \left[\left(\frac{\pi_t^\star}{\pi} \right) \left(\frac{\pi_t}{\pi_t^\star} \right)^{\phi_\pi} \left(\frac{\tilde{y}_t}{\tilde{y}_t^\star} \right)^{\phi_y} \right]^{1-\phi_r} \varepsilon_{r,t}, \tag{25}$$

(4) *Climate Change (CC) curve:*

$$m_t - m_{t-1} = \xi_m \sigma_t \left(1 - \tilde{\tau}_{e,t}^{\frac{1}{\theta_2 - 1}} \right) z_t l_t \tilde{y}_t \varepsilon_{e,t}. \tag{26}$$

In addition, the model includes *(i)* the following auxiliary variables:

$$\tilde{\lambda}_t = \varepsilon_{b,t} \left(\frac{x_t \tilde{y}_t - \omega \tilde{d}_t}{1-\omega} \right)^{-\sigma_c}, \tag{27}$$

$$x_t = 1 - (1-\vartheta)\frac{\kappa}{2}\left(\pi_t - \pi_t^\star\right)^2 - \theta_{1,t}\tilde{\tau}_{e,t}^{\theta_2/(\theta_2-1)}, \tag{28}$$

$$mc_t = \frac{\psi}{(1-\omega)^{\sigma_c+\sigma_n}} \frac{\left(x_t \tilde{y}_t - \omega \tilde{d}_t\right)^{\sigma_c} \tilde{y}_t^{\sigma_n}}{\epsilon_{b,t} \Phi\left(m_t\right)^{1+\sigma_n}} + \theta_{1,t}\tilde{\tau}_{e,t}\left[\theta_2 + (1-\theta_2)\,\tilde{\tau}_{e,t}^{\frac{1}{\theta_2-1}}\right], \tag{29}$$

where $\tilde{d}_t = d_t/z_t = d\Phi(m_t)$, and $\tilde{\tau}_{e,t} = \tau_{e,t}\sigma_t\varepsilon_{e,t}/(\theta_2\theta_{1,t})$, and *(ii)* five exogenous trends $\{z_t, \theta_{1,t}, l_t, \sigma_t, \pi_t^\star\}$ and four AR(1) shocks $\{\varepsilon_{b,t}, \varepsilon_{p,t}, \varepsilon_{r,t}, \varepsilon_{e,t}\}$.[12]

3. Bayesian inference

In this section, we estimate the model using Bayesian methods, using quarterly global data spanning from 1985Q1 to 2023Q2. The posterior distribution associated with the vector of observable variables is computed numerically using a Markov Chain Monte Carlo sampling approach.[13] Specifically, the Metropolis-Hastings algorithm enables efficient exploration of the high-dimensional parameter space, yielding a posterior distribution that quantifies uncertainty in parameter estimates arising from data limitations and model specification. Rather than relying on point estimates, this approach generates a distribution of plausible parameter values grounded in the data. This, in turn, allows us to assess how parameter uncertainty affects the model's main predictions and to report credible intervals around them. We begin by describing how the nonlinear model with trends is solved, followed by a discussion of the selected data and our choice of priors, before commenting on the posterior distribution of the structural parameters.

3.1. Numerical solution method with stochastic growth.

To solve the model, we address two key challenges: inherent nonlinearities in climate dynamics and unbalanced growth induced by five structural trends: rising population, output, and carbon emissions, alongside declining abatement efficiency and inflation targets.[14] We adapt the *extended path* solution method of Fair and Taylor (1983) and Adjemian and Juillard (2014) to account for the presence of growth in our model, avoiding the limitations of local solution techniques. The extended

[12] Appendix A in the Online Appendix provides the complete set of equations, including the shock processes and structural trends.

[13] We obtain a random draw of size 140,000 from the posterior distribution of the model parameters. This is achieved though 14 parallel chains, each running 10,000 iterations, with a common jump scale parameter calibrated to obtain an acceptance rate of approximately 30%).

[14] These trends are fundamental for accurately assessing climate change effects but render traditional perturbation methods unsuitable, as local approximations (e.g., around a deterministic steady state) break down.

path method relies on a perfect foresight solver to compute paths for endogenous variables consistent with the model's equations, given a sequence of exogenous MIT shocks and the absence of aggregate uncertainty. While the classical extended path assumes convergence to a fixed steady state once shocks dissipate, our implementation instead allows convergence to a nonstationary deterministic transition path, reflecting the persistent structural trends embedded in the model. The advantage of this method is that it delivers an accurate and computationally efficient solution while accounting for all model nonlinearities.[15]

Taking nonlinear models to the data presents challenges, as nonlinear filters, necessary for forming the likelihood function, are computationally demanding. The inversion filter offers a computationally efficient alternative (see Guerrieri and Iacoviello, 2017). Originally introduced by Fair and Taylor (1983), the inversion filter recursively extracts the sequence of innovations by inverting the observation equation, given a set of initial conditions. Unlike the Kalman or particle filters, it relies on an analytical characterization of the likelihood function.[16] The inversion filter extends the perfect foresight solution of Juillard (1996) through a modified implementation that recovers the sequence of errors consistent with observed data. Finally, we use the Metropolis-Hastings algorithm to sample from the posterior distribution and account for parameter uncertainty.[17]

3.2. **Data description.** As some time series are not available on a quarterly basis, appropriate transformations are required. First, annual GDP in constant 2015 US$ is sourced from the *World Bank* (https://short-link.me/11hzB) and quarterly interpolated using the method of Chow and Lin (1971). This procedure relies on real quarterly GDP for total OECD countries from the *OECD Economic Outlook* database (https://short-link.me/15rfm) as the high-frequency indicator.[18] Quarterly headline inflation (https://short-link.me/15reP) and short-term nominal interest rates (https://short-link.me/11hyb) are also taken from the *OECD Economic Outlook* database. The aggregate interest rate is constructed by weighting national interest rates by their respective shares of OECD GDP. Annual

[15] Appendix B in the Online Appendix provides additional details on the general representation of the perfect foresight algorithm in the presence of extended path, and the underlying statistical model used to estimate forward-looking models with structural changes.

[16] For a discussion of alternative filters for likelihood computation, see Fernández-Villaverde et al. (2016). See also Cuba-Borda et al. (2019) for detailed comparisons of inversion filter performance.

[17] The codes are part of a dedicated toolbox that builds on and extends the standard Dynare package (Adjemian et al., 2024), and are publicly available here: https://github.com/Vermandel/Climate-Economics-Dynare.

[18] This temporal disaggregation technique establishes a statistical relationship between low-frequency data and higher-frequency indicator variables. The method involves estimating regressions at the low-frequency level and applying the resulting coefficients to the indicator variables to construct a quarterly version of the target series.

CO_2 emissions, measuring emissions from fossil fuel combustion and cement production, are obtained from *Our World In Data* (https://short-link.me/11hzb). These data are also converted to quarterly frequency using the same Chow-Lin disaggregation approach applied to GDP. Standard macroeconomic estimation techniques typically require stationarity, achieved by dividing variables by population, detrending, or applying filters. By contrast, our solution method directly accommodates nonstationary data and does not rely on such transformations. Following standard practice in the estimation of structural models (e.g., Smets and Wouters, 2007), we express quantities in growth rates, although our approach could equally be applied to level data without difficulty.[19] The measurement equations linking the model to the four macroeconomic and climate-related times series are given by:

$$\begin{bmatrix} \text{Real output growth rate} \\ \text{Inflation rate} \\ \text{Short-term interest rate} \\ \text{CO}_2 \text{ emissions growth rate} \end{bmatrix} = \begin{bmatrix} \Delta \log (y_t) \\ \pi_t - 1 \\ r_t - 1 \\ \Delta \log (e_t) \end{bmatrix}. \tag{30}$$

3.3. **Calibrated parameters.** A first set of parameters is calibrated and can be grouped into two categories: structural parameters and initial conditions. We begin by discussing the calibration of the structural parameters, which are reported in Panels A and B of Table 1.

These parameters are categorized into three panels. Panel A pertains to the climate dynamics. The parameter ξ_m converts CO_2 to carbon units (GtC = ξ_m $GtCO_2$), ensuring consistency with climate damages measured in terms of cumulative carbon emissions. The parameter γ, which governs the impact of climate damages on total factor productivity (TFP), is set to 3.6×10^{-5}. This value implies a permanent 5% reduction in TFP under a business-as-usual scenario in 2100, in line with the recent calibration proposed by Barrage and Nordhaus (2024). This value is higher than that used in Golosov et al. (2014), reflecting the fact that damages in the DICE 2023 model (partly due to the inclusion of tipping risks and updated empirical estimates) are almost twice as large as in the 2016R2 version. [20] For the remaining parameters of the panel, we follow Barrage and Nordhaus (2024). The abatement cost function curvature, θ_2, is set to 2.6 to ensure strong convexity. Technological progress in the abatement sector, δ_{pb}, is calibrated to reduce abatement costs by 1.7% annually. In contrast, the decay rate of carbon decoupling δ_σ, is set to zero.

[19] Appendix C in the Online Appendix displays the times series of all observable variables used in the model.

[20] These damages likely represent a lower bound, as recent empirical evidence (e.g., Bilal and Känzig, 2024) points to substantially larger economic impacts of climate change. In the appendix, we report a robustness check in which we substantially raise this parameter to reflect this new evidence.

TABLE 1. Calibrated parameter values and initial conditions (quarterly basis)

NAME		VALUE	NAME		VALUE
Panel A: Climate parameters					
Atmospheric conversion factor	ξ_m	3/11	Long-term inflation target	$\pi^\star_\infty$	0.005
Climate damage elasticity	γ	3.57e-05	Decay TFP (annualized)	δ_z	0.0018
Abatement cost curvature	θ_2	2.6			
Decay abatement cost	δ_{pb}	0.017/4			
Decay rate emission intensity	δ_σ	0	**Panel C: Initial conditions**		
			Initial GDP (trillion USD PPP)	y_{t_0}	7.5
Panel B: Economic parameters			Initial inflation trend (annualized)	$\pi^\star_{t_0}$	12/400
Firm exit probability	ϑ	0.05	Initial emissions ($GtCO_2$)	e_{t_0}	5.075
Unemployed payoff-to-consumption	d/c	0.97	Initial abatement cost-to-gdp	θ_{1,t_0}	0.3191
Share low productive workers	ω	0.02	Initial population (billion)	l_{t_0}	4.85
Terminal population (billion)	l_∞	10.48	Initial stock of carbon (GtC)	m_{t_0}	720
Population growth	l_g	0.025/4	Initial carbon price ($/ton)	τ_{e,t_0}	0
Goods substitution elasticity	ζ	4	Initial hours worked	h_{t_0}	1

Note: $t_0 = 1984Q4$.

Panel B presents the calibration of the economic parameters. For discounting in the Euler and Phillips curves, the firm exit rate ϑ is set at 5%, consistent with the firm entry and exit literature and OECD data on firm death rates in the manufacturing and services sectors. In contrast, the Euler discount depends on the parameters ω and d. Following McKay et al. (2017), we calibrate the model to produce an effective discount rate of 3% by assuming that 2% of workers experience an income shock, and that insurance covers 97% of their consumption. Regarding population dynamics, the initial population at the start of the sample (1984Q4) is set at 4.85 billion. It is assumed to converge toward a long-term population level of $l_\infty = 10.48$ billion at an annual rate of 2.5%, consistent with United Nations projections for the year 2100. The substitutability across intermediate goods implies a 33% markup, a standard value in macroeconomic models featuring imperfect competition. Finally, the growth decay parameter δ_z is taken from the DICE 2023 model.

Panel C reports the initial conditions required to pin down all state variables of the model prior to estimation at $t_0 = 1984Q4$. Labor supply is normalized to one. For the exogenous inflation target process, we minimize the difference between the model and observed inflation data. This yields an initial inflation target of 12% annually, which decays toward a long-run target of 2%. To ensure realistic levels for GDP and CO_2 emissions, we set initial GDP to 7.5 trillion USD and emissions to 5 $GtCO_2$, in line with 1984 data. The initial values of population, GDP, interest rate, and emissions are all set to their observed levels in 1984Q4. Based on atmospheric carbon concentration data, we set the initial carbon stock m_{t_0} to 720 GtC. From these values, we compute the implied damages and calibrate the initial level of hours

worked to determine the disutility of labor parameter ψ. Given the initial GDP y_{t_0}, we use the production function to derive the initial level of total factor productivity, z_{t_0}. The level of the abatement cost function θ_{1,t_0} is calibrated following Barrage and Nordhaus (2024), who set abatement costs to reach 10.9% of GDP in 2020 under full abatement ($\mu = 1$). Since our simulation begins in 1984, we extrapolate this value backward, resulting in an estimated cost share of approximately 31.9% of GDP at t_0.

The final variable requiring discussion is the expected path of the carbon tax $\tilde{\tau}_{e,t}$. The out-of-sample transition scenario influences agents' expectations, which in turn affects the data representation captured by the estimated model. Rather than imposing an arbitrary mitigation path (such as strict adherence to the Paris Agreement), we allow the data to inform the expected carbon tax trajectory. Let $\{\tilde{\tau}^{\star}_{e,t}\}^{T}_{1984Q4}$ denote the benchmark carbon tax path consistent with temperature stabilization by 2050, as targeted in the Paris Agreement.[21] Recognizing that agents may not fully believe in the realization of this mitigation path, we introduce an expectation formation mechanism: $\mathbb{E}_t\{\tilde{\tau}_{e,t+s}\} = \varphi\tilde{\tau}^{\star}_{e,t+s}$, where $\varphi \in [0,1]$ captures the degree of belief in the policy scenario and s is a date in the future. The parameter φ can be interpreted as *(i)* the prior probability that the mitigation policy will be fully implemented, *(ii)* the fraction of agents who believe in the policy's realization, or *(iii)* the perceived stringency of the policy path.

3.4. **Prior and posterior distributions.** The remaining parameters are estimated using priors reported in Table 2. For most structural and policy parameters, we follow the specification in Smets and Wouters (2007). The autoregressive coefficients of the shock processes are assigned Beta priors with a mean of 0.5 and a standard deviation of 0.1, providing a relatively informative prior. The prior for the labor supply elasticity parameter, σ_h, is taken directly from Smets and Wouters (2007) and specified as a Gamma distribution to ensure positivity. Similarly, the risk aversion parameter σ_c is given a Gamma prior with a mean of 1 and a standard deviation of 0.5. The Rotemberg price adjustment cost parameter κ uses a Gamma prior (mean 30, standard deviation 6), which is at the lower end of the range found in the literature. For the inflation reaction coefficient, a Gamma prior is imposed on $\phi_\pi - 1$ to satisfy the Taylor principle, and the output gap reaction coefficient ϕ_y is also assigned a relatively tight

[21] Formally, the Paris Agreement-consistent tax path is assumed to increase linearly from 2023Q3 to 2050Q1, starting at 0$ per ton of carbon and reaching 152$ per ton, consistent with the backstop price under a full mitigation policy. After 2050, the carbon price declines endogenously due to decreasing cost of abatement $\theta_{1,t}$ and carbon intensity σ_t, consistent with the DICE framework.

TABLE 2. Prior and posterior distributions of structural parameters

		Prior Distribution			Posterior Distribution		
		Shape	Mean	Std	Mode	Mean	[5%:95%]
Panel A: Shock processes							
Standard deviation: preference shock	σ_b	$\mathcal{IG}_2$	0.002	0.0033	0.024	0.0239	*[0.0205:0.027]*
Standard deviation: price markup shock	σ_p	$\mathcal{IG}_2$	0.002	0.0033	0.0147	0.0145	*[0.0126:0.0168]*
Standard deviation: monetary policy shock	σ_r	$\mathcal{IG}_2$	0.002	0.0033	0.0008	0.0008	*[0.0007:0.0009]*
Standard deviation: carbon emission shock	σ_e	$\mathcal{IG}_2$	0.002	0.0033	0.005	0.005	*[0.0045:0.0055]*
Autocorrelation: preference shock	ρ_b	$\mathcal{B}$	0.5	0.1	0.6665	0.6744	*[0.6301:0.714]*
Autocorrelation: price markup shock	ρ_b	$\mathcal{B}$	0.5	0.1	0.987	0.9849	*[0.9758:0.992]*
Autocorrelation: monetary policy shock	ρ_r	$\mathcal{B}$	0.5	0.1	0.4531	0.4675	*[0.4243:0.5162]*
Autocorrelation: carbon emission shock	ρ_e	$\mathcal{B}$	0.5	0.1	0.9607	0.9611	*[0.9461:0.9746]*
Panel B: Structural parameters							
Initial TFP growth	$g_{z,t_0} \times 400$	$\mathcal{G}$	1.5	0.5	1.9082	1.9132	*[1.8811:1.945]*
Decay rate decoupling	$g_{\sigma,t_0} \times 400$	$\mathcal{G}$	1.5	0.5	1.3163	1.3228	*[1.2598:1.396]*
Risk aversion	σ_c	$\mathcal{G}$	1	0.2	1.4056	1.4069	*[1.2132:1.5648]*
Labor disutility	σ_h	$\mathcal{G}$	2	0.25	0.8739	0.8517	*[0.7247:0.9477]*
Rotemberg Cost	κ	$\mathcal{G}$	30	6	145.1832	142.1713	*[127.1989:154.8274]*
Convergence rate of inflation target	$\rho_{\pi^\star}$	$\mathcal{B}$	0.02	0.01	0.0393	0.0397	*[0.0324:0.049]*
Initial interest rate	$r_{t_0} \times 400$	$\mathcal{N}$	15	2	8.8048	8.6982	*[8.1428:9.1281]*
Monetary policy: inflation	$(\phi_\pi - 1)$	$\mathcal{G}$	0.8	0.07	0.4191	0.42	*[0.3676:0.4749]*
Monetary policy: output gap	ϕ_y	$\mathcal{G}$	0.04	0.005	0.0606	0.0613	*[0.0487:0.0699]*
Monetary policy: smoothing	ρ	$\mathcal{B}$	0.75	0.05	0.8827	0.8784	*[0.8561:0.8997]*
Discount rate	$(\beta^{-1} - 1) \times 100$	$\mathcal{G}$	0.8	0.2	0.2009	0.2019	*[0.1696:0.229]*
Mitigation policy belief	φ	$\mathcal{B}$	0.5	0.2	0.4522	0.4538	*[0.3882:0.5308]*
Log marginal data density							-2897.3

Note: $\mathcal{B}$ denotes the Beta, $\mathcal{G}$ the Gamma, $\mathcal{N}$ the Gaussian, and $\mathcal{IG}_2$ the Inverse Gamma (type 2) distributions. A total of 120,000 draws were used to compute the posterior mean and 90% confidence interval. $t_0 = 1985Q4$.

Gamma prior. The exogenous shocks are specified to follow an inverse gamma type 2 distribution, as in Christiano et al. (2014), with a prior mean of 0.002 and a standard deviation of 0.0033. The annualized slopes of TFP growth and carbon decoupling are estimated using diffuse Gamma priors (mean 1.5, standard deviation 0.5), consistent with values typically found in DICE models. Finally, the mitigation belief probability φ is assigned a diffuse Beta prior with a mean of 0.5 and a standard deviation of 0.2, capturing a wide range of possible beliefs regarding policy credibility.

We next examine the posterior distributions generated by the Metropolis-Hasting sampler, reported as 90% confidence intervals in Table 2. The price mark-up shock exhibits the highest persistence, consistent with the findings of Smets and Wouters (2007). Notably, the pollution shock also shows substantial persistence, in line with the results of Jondeau et al. (2025). Initial productivity growth is estimated to be higher than typical values in DICE models. This is expected, given that our simulation begins in 1985, a period characterized by stronger TFP growth compared to the 2015-2020 window used in DICE. A similar pattern is observed for the carbon decoupling rate. Relative to Smets and Wouters (2007), our estimates imply a flatter labor supply curve, which in turn flattens the marginal cost schedule and dampens the

sensitivity of inflation to fluctuations in hours worked. Additionally, the Rotemberg price adjustment cost parameter is estimated to be relatively high, indicating a relatively flat Phillips curve. This finding aligns with extensive evidence from the Great Moderation period. The estimated coefficients on Taylor rules are effectively in line Smets and Wouters (2007). Importantly, the model estimates that agents assigned a probability of approximately 45% to achieving the goals of the Paris Agreement.

Model evaluation– An evaluation of the model's fit is provided in Appendix D of the Online Appendix. It includes *(i)* a comparison of empirical and model-implied moments, *(ii)* generalized impulse response functions for the four shocks, *(iii)* a comparison of model-implied and reduced-form impulse responses to a carbon price shock, and *(iv)* a historical decomposition of detrended output, inflation, and the nominal interest rate. Overall, the model captures the empirical dynamics of these key variables reasonably well and successfully replicates the empirical evidence on the effects of a carbon price shock.

Long-term projection exercices– In what follows, our analysis partly relies on long-term projections generated by the model to explore alternative trajectories for the global economy up to 2100. Specifically, we assume that in 2023Q3, agents receive information about the long-term carbon tax path, which may involve a surprise change in policy intensity. We begin by considering an optimal policy path based on the social cost of carbon. In this scenario, the carbon tax follows its welfare-maximizing trajectory, derived from the model's optimality conditions and balancing mitigation costs with long-term climate damages. We then focus on two alternative scenarios that differ solely in the degree of effective policy implementation, captured by the parameter φ. The first scenario represents full implementation of the *Paris Agreement* ($\varphi = 1$), implying a carbon tax consistent with achieving net-zero emissions by 2050. The second assumes that agents learn no carbon tax will be enacted ($\varphi = 0$), leading to continued emissions growth (*laissez-faire*). In both cases, agents revise their expectations following a policy surprise.

These projections are driven by four main forces that differ markedly from the standard shock analyses in New Keynesian models: *(i)* exogenous processes, based on their in-sample realizations; *(ii)* deterministic trends gradually converging to terminal states; *(iii)* the implemented carbon price policy; and *(iv)* the accumulation of atmospheric carbon, which imposes permanent economic damages. Far from being purely illustrative, these simulations constitute genuine out-of-sample forecasts generated by a structurally estimated dynamic model. This approach ensures internal consistency by anchoring both structural parameters and initial conditions in the data.

4. Nominal Rigidities and the Social Cost of Carbon

The social cost of carbon (SCC) represents the monetary value of the economic damage caused by emitting one additional ton of carbon dioxide into the atmosphere. It thus provides the theoretically optimal price of carbon emissions and serves as a key benchmark for policy evaluation and model comparison. In this section, we *(i)* analyze how nominal rigidities affect the SCC, *(ii)* examine the aggregate consequences of carbon mispricing that arise when nominal rigidities are ignored, and *(iii)* explore the macroeconomic implications of aligning carbon pricing with this optimal trajectory.

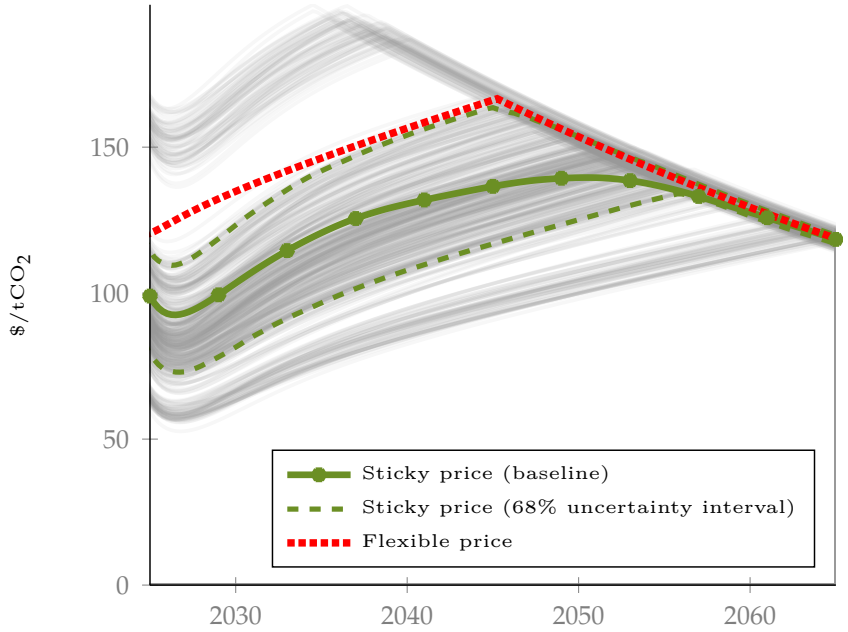
4.1. **Pricing carbon in the presence of sticky prices.** We first assess whether nominal price rigidities significantly affect the determination of the socially optimal carbon price. An approximation of the SCC can be formally expressed as:

$$SCC_t \approx \beta \mathbb{E}_t \left\{ \frac{\tilde{\lambda}_{t+1}}{\tilde{\lambda}_t} SCC_{t+1} + 1000 \xi_m \frac{l_{t+1} z_{t+1}}{\tilde{\lambda}_t} \gamma \psi \left(\frac{n_{t+1}}{1-\omega} \right)^{1+\sigma_n} \right\}, \tag{31}$$

In this equation, $\gamma\psi \left(n_{t+1}/\left(1-\omega\right)\right)^{1+\sigma_n}$ captures the marginal damage, and as a reminder, $\tilde{\lambda}_t = \varepsilon_t^b \left(\frac{x_t \tilde{y}_t}{1-\omega} - \omega \tilde{d}_t \right)^{-\sigma_c}$ is the (detrended) marginal utility of consumption, which is used to express the SCC in consumption-equivalent terms. Finally, x_t denotes the resources available for consumption after accounting for costs induced by both inflation and abatement efforts. This formulation is closely related to Golosov et al. (2014), with the key difference that nominal rigidities matter. In our framework, the welfare cost of inflation appears directly through its impact on the marginal utility of consumption, which serves as the intertemporal pricing kernel.

When realized inflation persistently exceeds the central bank's target, particularly as a result of carbon taxes generating additional inflationary pressure, this amplifies the welfare cost of inflation by reducing x_t and, consequently, lowers agents' perceived wealth. In economic terms, the welfare cost of inflation manifests not only as a direct resource cost in the resource constraint, but also through its effect on the marginal utility channel: as agents feel poorer, their valuation of future welfare gains from abatement diminishes. Our analysis connects to Bailey (1956) and Lucas (2000), but it also resonates with insights from the fiscal theory of the price level (Leeper, 1991; Woodford, 1995; Cochrane, 2001). In contrast to standard monetary models where inflation is driven by monetary expansions, here inflation is primarily fiscal in origin, arising from persistent tax-induced shifts in the intertemporal government budget constraint. Accordingly, the welfare cost of "greenflation" has direct implications not only for monetary policy credibility, but also for the optimal path and timing of carbon pricing.

FIGURE 1. Pricing carbon at its social cost



Note: This figure depicts carbon tax set to the social cost of carbon as derived from the estimated New Keynesian Climate model (green line) alongside its flexible-price (natural) counterpart (red dotted line). Uncertainty bands for the baseline, based on 500 simulations with alternative parameter draws from the Metropolis-Hastings algorithm, are shown as solid gray lines.

In Figure 1, we report the optimal carbon price in both the sticky-price and flexible-price (or natural) economies, as well as uncertainty bands from 500 Metropolis-Hastings draws.[22] Once the transitory effect of shocks has dissipated, one observes that the optimal carbon tax is markedly higher in the flexible-price economy. In the absence of nominal rigidities, the transition is not accompanied by persistent inflation, and the welfare cost of inflation remains limited. By contrast, under sticky-prices, the social cost of carbon embodies a trade-off between nominal stability and climate objectives. If inflation is not stabilized during the green transition, the increased welfare cost of inflation diminishes the incentive for strong carbon

[22] Benchmarking our results against Barrage and Nordhaus (2024), we find that the level of the optimal carbon price in our model is broadly consistent with their main findings. However, direct comparison is complicated by important differences in model structure: our framework features behavioral discounting, nominal rigidities, imperfect competition, no physical capital. As a result, the main source of persistence in our model is interest rate smoothing, which allows the optimal carbon tax to converge more rapidly to the SCC. In contrast, Barrage and Nordhaus (2024) show that additional frictions result in a more gradual adjustment of the optimal carbon price toward the SCC. In our simulations, the optimal carbon price rises steadily and typically reaches the backstop price by 2060 in most Metropolis-Hastings draws. Our estimated carbon price also tends to be higher on average, reflecting our lower discount rate of 0.88%, which is estimated from global data and is lower than typical values used in DICE. This lower discount rate induces the planner to adopt a more aggressive carbon tax policy, accelerating the response to the climate externality. It is also worth noting that, across simulation draws, the optimal carbon price spans a wide range, from $50 to $160, encompassing the values reported in DICE and reflecting uncertainty associated with the estimated discount rate.

pricing and thus lowers the optimal SCC. In other words, optimal climate policy becomes less ambitious whenever the transition generates sustained inflation above target, because agents discount future climate damages more heavily when their perceived wealth is eroded by inflationary distortions.

4.2. **The aggregate implications of carbon mispricing.** Standard IAMs, including those used by the IPCC, are typically constructed in a real framework that abstracts from nominal frictions such as sticky prices and monetary policy dynamics. As a result, the optimal SCC recommended by these models does not account for inflation or the welfare cost of inflation induced by carbon pricing.[23] In real-world policy settings, the SCC is thus computed from models that do not incorporate nominal rigidities. This raises an important question: what are the quantitative implications of applying such a mis-specified SCC in economies where nominal rigidities matter? To address this, we compute the SCC under both flexible-price and sticky-price environments. We then assess the macroeconomic implications of implementing a mis-specified SCC: specifically, applying an SCC derived under flexible-price assumptions (red dotted line in Figure 1) in an economy where nominal rigidities distort the transmission of climate policy.

We quantify the costs of such miscalibration along two key dimensions. First, we compare aggregate consumption paths under two regimes: one based on the flexible-price SCC and the other on the SCC optimized for the sticky-price environment (green line in Figure 1). The resulting difference, expressed in monetary terms (billions of dollars), reflects the real economic cost borne by households due to mispriced carbon tax. Second, we assess the inflation outcomes under both regimes to evaluate how a misaligned SCC impacts price stability. This comparison reveals the extent to which nominal rigidities amplify the inflationary effects of an ill-suited climate policy.

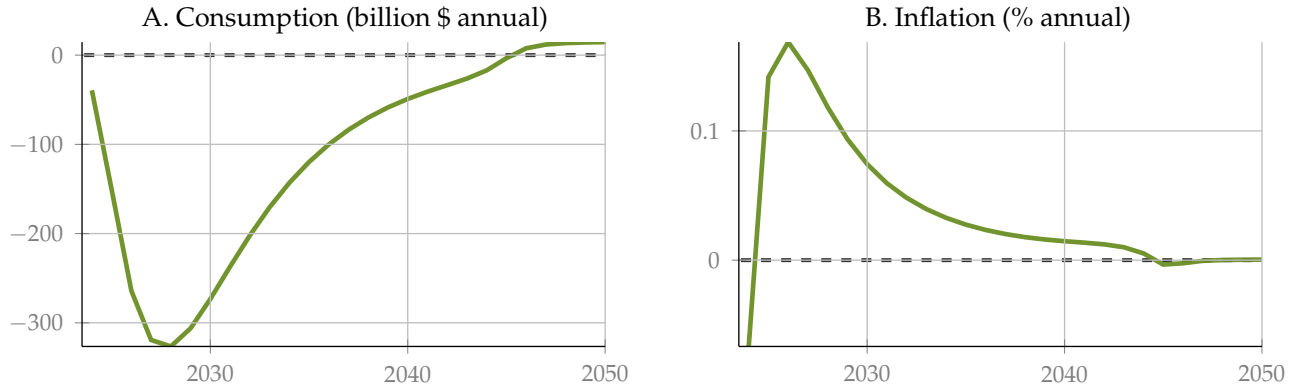
As shown in Figure 2, there are two main losses from applying an SCC derived from a flexible-price framework. It results in an average consumption loss of approximately $110 billion per quarter through 2050, with losses peaking at $326 billion just before 2030. These figures are economically significant. On the inflation side, the average deviation is 0.04 percentage points, with short-term differences reaching nearly 0.2 percentage points in annualized terms.[24] These results illustrate how the welfare cost of inflation materializes in this

[23]For example, the Biden administration in the United States set its central SCC at $52 per ton, based on a multi-model average derived from five leading IAMs. All of these models neglect inflationary effects and the welfare cost of inflation.

[24]The inflationary effects reported here should be interpreted in light of the assumption of Rotemberg-style quadratic price adjustment costs. Future work could explore alternative nominal rigidity specifications, such as menu cost models, in which firms adjust prices only when the expected benefit exceeds a fixed adjustment cost.

context. Because nominal rigidities slow the adjustment of prices, the economy is forced to absorb shocks primarily through quantities such as consumption and output, rather than through prices. This effect is especially pronounced when the SCC is calibrated from a natural (flexible-price) economy, as it does not account for the nominal distortions present in the real world. As a result, ignoring these nominal effects can lead to substantial welfare losses during the low-carbon transition.

FIGURE 2. Macroeconomic costs of mispricing the social cost of carbon



These findings have important policy implications. Nominal rigidities play a central role in shaping the macroeconomic consequences of carbon pricing. Yet current policy recommendations often rely on social cost of carbon estimates derived from models that abstract from these frictions. This oversight can weaken the effectiveness and public acceptance of climate policies. Recent episodes, such as the "yellow vest" protests in France, illustrate how public support for higher carbon prices can erode when such measures are perceived as fueling inflation and worsening cost-of-living conditions. Survey evidence confirms that individuals have a strong aversion to inflation and view its distributional effects as particularly unfair (Shiller, 1997; Di Tella et al., 2001), which can intensify opposition to climate interventions (Dechezleprêtre et al., 2025).

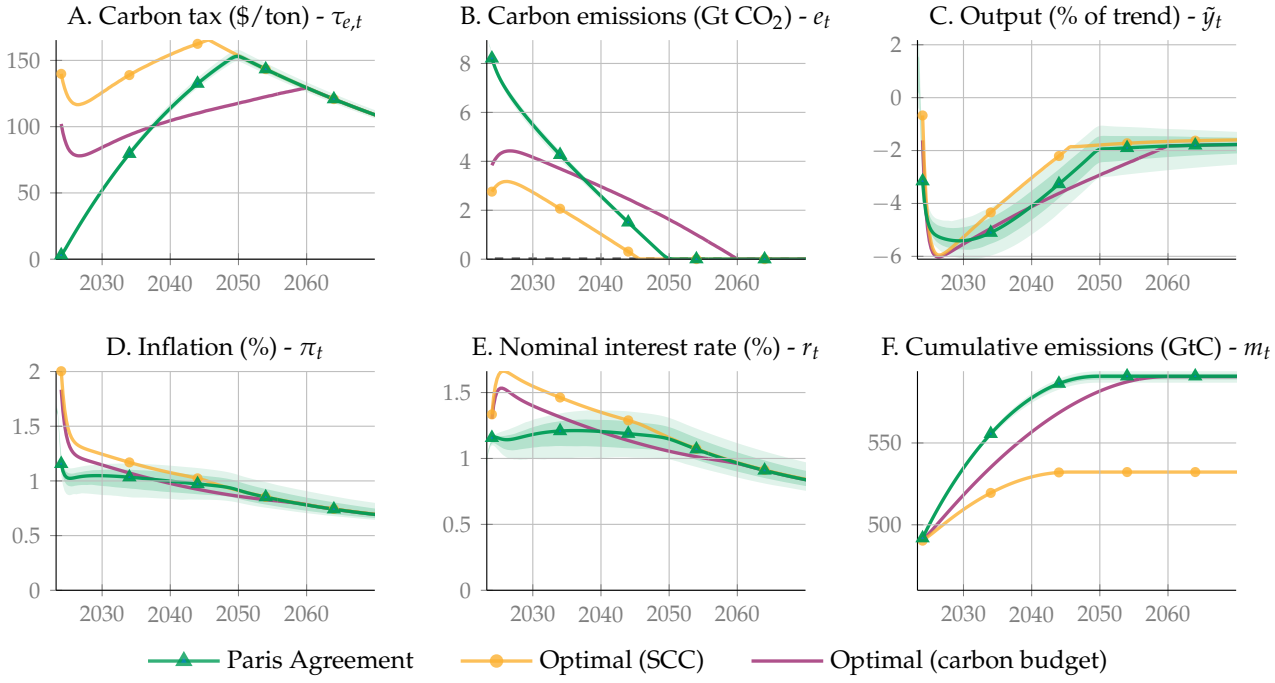
4.3. **The macroeconomic implications of adhering to optimal transition pathways.** In the Paris Agreement scenario, the tax path is imposed exogenously rather than optimally adjusted to maximize social welfare. Consequently, this approach is not directly comparable to integrated assessment models such as DICE, where the carbon price is determined endogenously to balance economic and environmental tradeoffs. To establish a more meaningful

Such models typically generate less price dispersion by limiting how far prices drift from their optimal levels (Nakamura et al., 2018).

benchmark, we therefore compare the Paris Agreement carbon trajectory with two alternative optimal pathways: one based on the social cost of carbon, and another based on the optimal exhaustion of a fixed carbon budget. Under the Paris Agreement scenario, the atmospheric carbon stock is projected to increase by 100 GtC by 2050. For comparability with the scenario in Barrage and Nordhaus (2024), which targets limiting global warming to below 2°C, we also examine an alternative pathway in which a 100 GtC carbon budget is exhausted optimally over time.[25]

Figure 3 compares the evolution of key macroeconomic and environmental variables under three distinct policy scenarios: *(i)* the Paris Agreement (green line), *(ii)* a carbon tax path aligned with the SCC (yellow line), and *(iii)* a carbon tax path consistent with the carbon-budget rule (purple line).

FIGURE 3. Alternative carbon tax trajectories



Note: This figure presents the projected paths of key macroeconomic and environmental variables under two scenarios within the New Keynesian climate model: *(i)* the Paris Agreement scenario, which assumes a carbon tax consistent with achieving net-zero emissions by 2050, and *(ii)* the optimal tax trajectory scenario, which reflects the optimal exhaustion of a fixed carbon budget. The green area denotes the uncertainty band associated with the Paris Agreement scenario, obtained from 500 random draws generated using the Metropolis-Hastings sampler.

[25] The extraction rate for this scenario follows the optimal path defined by:

$$\max_{\{s_t\}} \mathbb{E}_t \left\{ \sum_{s=0}^{\infty} \tilde{\beta}_{t,t+s} \left(\frac{c_{t+s}^{1-\sigma_c} - 1}{1-\sigma_c} - \psi_{t+s} \frac{n_{t+s}^{1+\sigma_n}}{1+\sigma_n} \right) \right\} \quad \text{s.t.} \quad \Delta s_t = -\xi_m e_t.$$

This defines the optimal depletion path of the carbon stock s_t, subject to emissions e_t, and implies an alternative trajectory for the carbon tax consistent with optimal budget exhaustion.

The optimal SCC path features a high initial carbon price, which drives a rapid decline in emissions, reaching net zero by around 2045, earlier than both the Paris Agreement and carbon budget paths. As a result, it also achieves the lowest cumulative emissions, approximately 58 GtC lower than in the other scenarios. Economically, the SCC path entails a larger short-run drop in output due to the strong initial tax shock, but this is followed by a more robust long-run recovery, reflecting the benefits of early mitigation. In addition, inflation is higher under the SCC scenario in the near term, as the steep initial rise in carbon prices feeds through to production costs and consumer prices. The carbon budget path, by contrast, also begins with a high initial carbon tax, though lower than under the SCC, and its subsequent increase is more gradual. It suggests that deferring net-zero emissions beyond 2050 is welfare-optimal, with net zero reached around 2060. This outcome reflects the economic cost structure of abatement, whereby eliminating the final units of emissions is disproportionately expensive. Hence, an intertemporally optimal strategy involves postponing some abatement efforts, anticipating future declines in abatement costs. Finally, the Paris Agreement path reaches net zero by 2050, following a smoother and more policy-guided trajectory. Overall, the SCC trajectory delivers the most effective and timely emissions reduction, albeit with greater short-term economic adjustment costs.

5. The anatomy of greenflation and climateflation

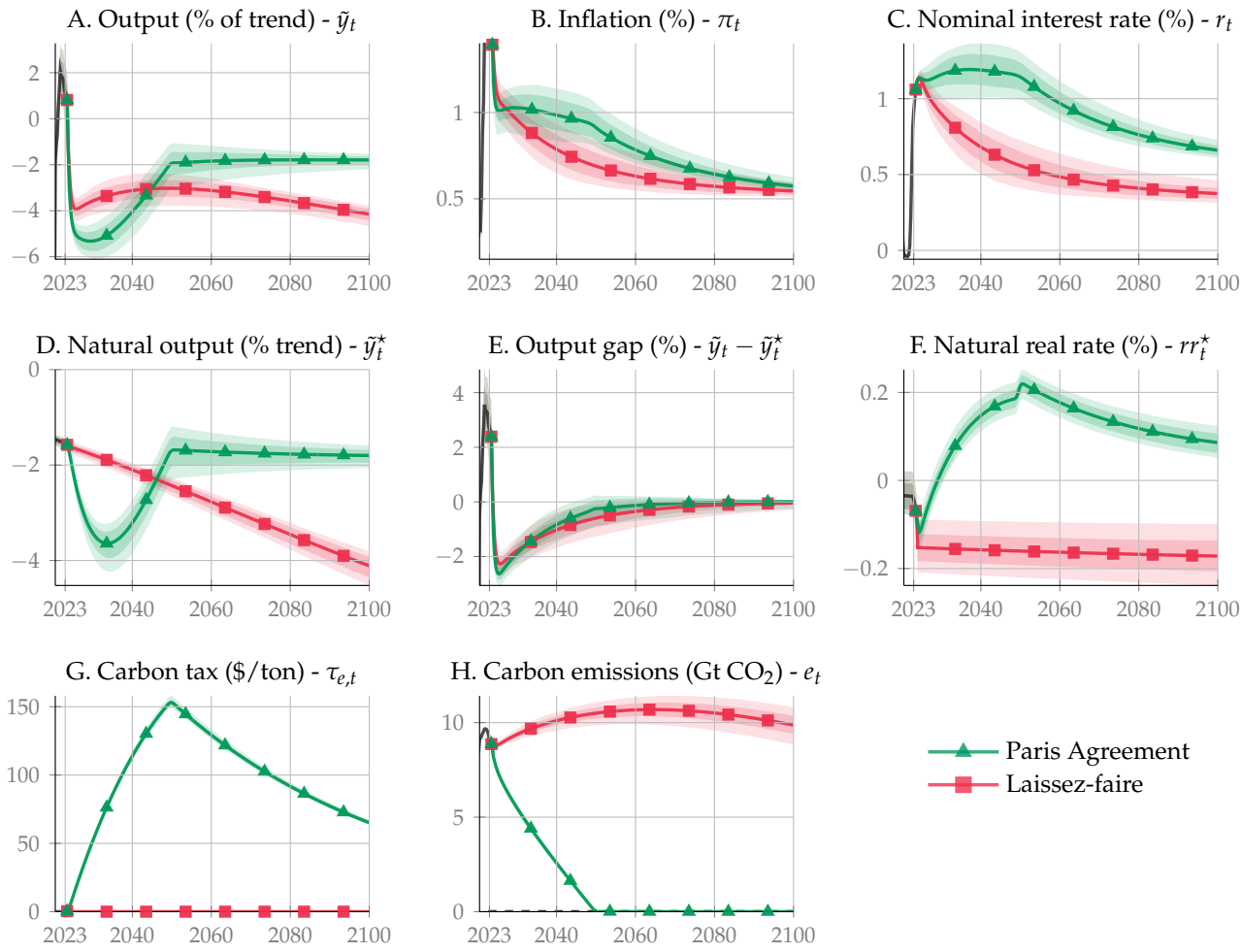
In this section, we analyze how the phenomena of climateflation and greenflation may influence the global economy through 2100. We begin by presenting long-term projections from the model to illustrate potential trajectories for the global economy by 2100. We then decompose output and inflation into their macroeconomic and environmental components to identify the key drivers of the transition.

5.1. **Long-term projections under three CO2 emission scenarios.**

Figure 4 shows the results for the two aforementioned scenarios: *laissez-faire* (red) and *Paris Agreement* (green).

In the absence of emission controls and with a zero carbon tax, the laissez-faire scenario leads to a continuous increase in climate damages, driven by the ongoing rise in cumulative emissions. This leads to a progressive decline in total factor productivity, natural output (Panel D), and the natural real interest rate (Panel F). Although the economy begins recovering from the energy price shock recession in 2023, output soon falls below the technological neutral trend due to intensifying climate damages, causing GDP to decline by nearly 4%

FIGURE 4. Model-implied projections based on alternative control rates of emissions



Note: This figure reports the projected paths of the main variables in the New Keynesian climate model under two scenarios: *(i)* the Paris Agreement, with a carbon tax consistent with achieving net zero emissions by 2050, and *(ii)* laissez-faire, with no carbon tax. Shaded areas denote the uncertainty bands associated with the Paris Agreement (green) and laissez-faire (red) scenarios, obtained from 500 random draws generated using the Metropolis-Hastings sampler.

relative to trend (Panel A). The anticipated weakening of demand further suppresses inflation (Panel B), pushing it below the baseline blue scenario.[26] In response, the central bank lowers the policy interest rate (Panel C). Recent empirical work further highlights the supply-side origins of climateflation. Baleyte et al. (2024) show, using long-run historical data, that climate-related shocks tend to raise inflation and dampen economic activity, much like classic supply shocks.

The economy evolves quite differently under the Paris Agreement scenario. Here, a gradually increasing carbon tax is implemented, reaching $150 per ton of CO_2 emissions by 2050,

[26]Climate damages act as a persistent supply shock, an effect extensively studied in Nuño et al. (2024) with respect to monetary policy.

sufficient to support the transition to a net-zero carbon economy (Panels G and H). Initially, natural output declines due to the rising tax burden and associated abatement costs. However, as abatement expenditures stimulate aggregate demand, output subsequently rises and converges to a level around 2% below trend, reflecting the irreversible effect of cumulative emissions in the atmosphere, which permanently depress total factor productivity. The natural real interest rate follows a qualitatively similar pattern (Panel F). One notable consequence of this investment-led recovery is the emergence of more persistent inflationary pressures. The output gap closes gradually under the Paris Agreement path (Panel E), as under the laissez-faire scenario.

Importantly, inflationary pressures persist even after net-zero is achieved in 2050. This reflects the continued economic costs associated with abatement investments, as captured in the DICE framework. These costs are modeled as flow expenditures, implicitly representing the amortized net present value of decarbonization efforts over the lifetime of the deployed capital or technology. The combined effects of rising carbon taxes and increased abatement-driven demand generate a sustained inflationary impulse, a phenomenon we refer to as "greenflation". Consequently, monetary policy must tighten (Panel C) to manage these inflationary pressures. This result is supported by Fornaro et al. (2025), which show that accounting for endogenous technological change deepens the green dilemma for central banks: tolerating temporary inflation risks unanchoring expectations, while strict inflation targeting raises the economic cost of the transition by suppressing green investment and slowing progress toward sustainability. On empirical grounds, the inflationary effects of carbon taxation have been documented by Känzig and Konradt (2024) in the European context. The study finds that carbon taxes operate much like supply shocks, leading to higher inflation and a decline in real activity. This empirical evidence corroborates our findings regarding the emergence of greenflation in response to climate mitigation policies.

The deliberate simplicity of our model allows us to exploit its tractability to disentangle the most salient mechanisms that shape the transition. In particular, we perform a decomposition of aggregate demand and supply to identify the macroeconomic and environmental forces driving the dynamics of output and inflation, features common to a broad class of environmental macroeconomic models

5.2. **Decomposing output.** In this section we analyze the various forces that influence total output. From the resource constraint, the logarithm of detrended output, defined as $\hat{y}_t =$

$\log(\tilde{y}_t/\tilde{y})$ can be approximated as follows:[27]

$$\hat{y}_t \simeq \underbrace{\widehat{IS}_t}_{\text{consumption}} + \underbrace{\theta_{1,t}\tilde{\tau}_{e,t}^{\theta_2/(\theta_2-1)}}_{\text{abatement expenditures}} + \underbrace{\frac{\kappa}{2}(\pi_t - \pi_t^\star)^2}_{\text{nominal costs}}. \tag{32}$$

Three main forces can be identified in the decomposition of output. The first is $\widehat{IS}_t$, which captures the standard permanent income and intertemporal substitution effects on **consumption**.[28] This term also embodies the primary channel through which monetary policy operates. However, relative to the standard New Keynesian framework, its effect is attenuated due to the presence of discounting in the Euler equation. The second term represents **abatement expenditures**, autonomous abatement investment required to meet net-zero emission targets by 2050. These expenditures act as a source of aggregate demand, independent of monetary or fiscal stimulus. The third component, labeled **nominal costs**, reflects the resource costs associated with price adjustment.

Figure 5 presents a decomposition of detrended output into three components across these scenarios. Note that Panel A shows total detrended output, which is the sum of the components shown in Panels B, C, and D. Under the Paris Agreement scenario, the rise in carbon taxes initially induces a deeper recession relative to the baseline, followed by a pronounced economic expansion as abatement spending intensifies, peaking at over 4% of output during the transition and then gradually declining thereafter.[29] This initial downturn is primarily driven by negative supply-side effects, as higher taxes crowd out consumption (Panel B). In response to inflationary pressures arising from increased tax-induced production costs, monetary policy tightens. Notably, the inflationary burden (Panel D) remains relatively similar across all three scenarios and quantitatively negligible.

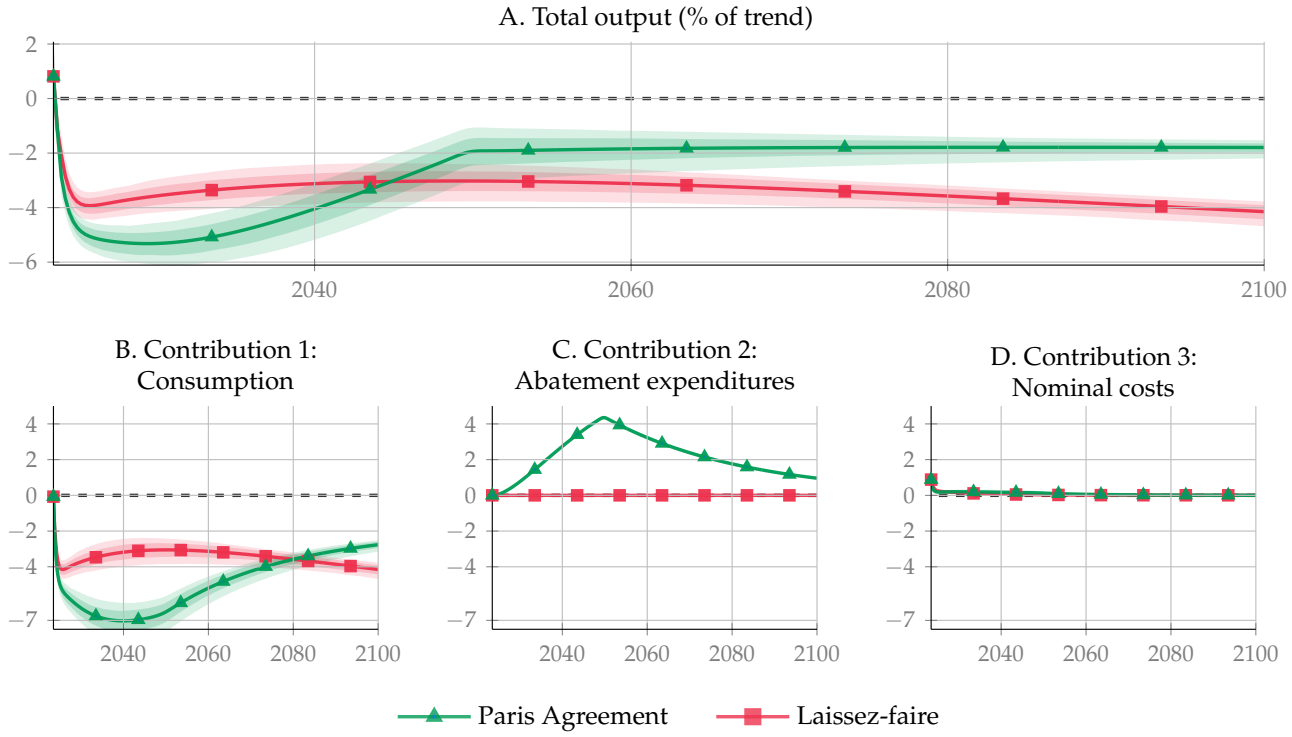
Conversely, the laissez-faire scenario yields a milder initial recession, as the absence of current and expected carbon taxes temporarily boosts output. Over time, however, rising

[27] Appendix E in the Online Appendix outlines the mathematical derivation of this approximation in detail.

[28] The attenuated IS has contribution $\widehat{IS}_t = \log(IS_t/IS)$ where attenuation coefficient $\omega \in [0,1]$ is given by $IS_t = \omega\tilde{d}_t + (1-\omega)\left[\omega\mathbb{E}_t\left\{\sum_{s=0}^{\infty}\beta(1-\omega)^s\varepsilon_{b,t+s}\tilde{d}_{t+s}^{-\sigma_c}\prod_{j=0}^{s}\frac{r_{t+j}}{\pi_{t+1+j}}\right\}\right]^{-1/\sigma_c}$.

[29] This persistence of abatement costs reflects the structure of marginal abatement cost (MAC) curves, aligned with the DICE framework. In the model, these costs are represented as the net present value of mitigation investments that are implicitly distributed over time. Economically, this is akin to a stream of coupon payments: even after the initial investment reduces emissions, firms continue to incur annual costs over the lifetime of the deployed capital or technology. Hence, abatement spending remains positive beyond the point of achieving net zero.

FIGURE 5. Decomposition of detrended output during the transition



Note: This figure reports the projected paths of the main variables in the New Keynesian climate model under two scenarios: *(i)* the Paris Agreement, with a carbon tax consistent with achieving net zero emissions by 2050, and *(ii)* laissez-faire, with no carbon tax. Shaded areas denote the uncertainty bands associated with the Paris Agreement (green) and laissez-faire (red) scenarios, obtained from 500 random draws generated using the Metropolis-Hastings sampler.

climate damages reduce productivity, pushing output below baseline. Anticipating this deterioration in future economic conditions, forward-looking agents cut consumption in favor of precautionary savings, dampening inflation. Here, climate change transmits to output mainly through the intertemporal IS channel.

5.3. **Decomposing inflation.** In the same spirit, we decompose the inflation gap, defined as $\hat{\pi}_t = \pi_t - \pi_t^\star$, into four main drivers:

$$\hat{\pi}_t \simeq \underbrace{\hat{\pi}_t^w}_{\text{real wage}} + \underbrace{\hat{\pi}_t^c}_{\text{climateflation}} + \underbrace{\hat{\pi}_t^g}_{\text{greenflation}} + \underbrace{\hat{\pi}_t^x}_{\text{cost-push shock}} . \tag{33}$$

To derive this decomposition, and owing to the strong nonlinearity of the Phillips curve, we apply a Shapley-value decomposition to both *(i)* Equation (24), which can be rewritten

as:[30]

$$(\hat{\pi}_t + \pi_t^\star)\hat{\pi}_t = \mathbb{E}_t \left\{ \sum_{s=0}^{+\infty} \beta_{t,t+s}^{\pi} \left(\frac{1-\zeta}{\kappa} + \frac{\zeta}{\kappa} mc_{t+s} \right) \right\}, \tag{34}$$

where $\beta_{t,t+s}^{\pi} = ((1-\vartheta)\beta)^s \left(\tilde{\lambda}_{t+s}\tilde{y}_{t+s}z_{t+s}\right) / \left(\tilde{\lambda}_t \tilde{y}_t z_t\right)$ is the discount factor adjusted by GDP growth, and *(ii)* Equation (29):[31]

$$mc_t = \underbrace{\left(\frac{\psi \left(x_t \tilde{y}_t - \omega \tilde{d}_t \right)^{\sigma_c} \tilde{y}_t^{\sigma_n}}{(1-\omega)^{\sigma_c + \sigma_n}} \right.}_{mc_t^w} \underbrace{\left. \frac{1}{\Phi \left(m_t \right)^{1+\sigma_n}} \right)}_{mc_t^c} + \underbrace{\tilde{\tau}_{e,t}\theta_{1,t} \left(\theta_2 + \tilde{\tau}_{e,t}^{\frac{1}{\theta_2 - 1}} \left(1 - \theta_2 \right) \right)}_{mc_t^g} \underbrace{\varepsilon_t^p}_{mc_t^x} \tag{35}$$

The component mc_t^w corresponds to the standard real-wage channel in marginal cost, as in Galí (2008), operating through general equilibrium interactions between wages and output. The term mc_t^c captures the impact of climate damages: rising emissions reduce total factor productivity, thereby increasing production costs. The component mc_t^g reflects the effect of carbon taxation and associated abatement efforts, introducing an additional source of cost pressure on firms. This term is exogenous in our setup, depending only on the extent of carbon tax implementation. Finally, mc_t^x represents the conventional cost-push shock affecting inflation.

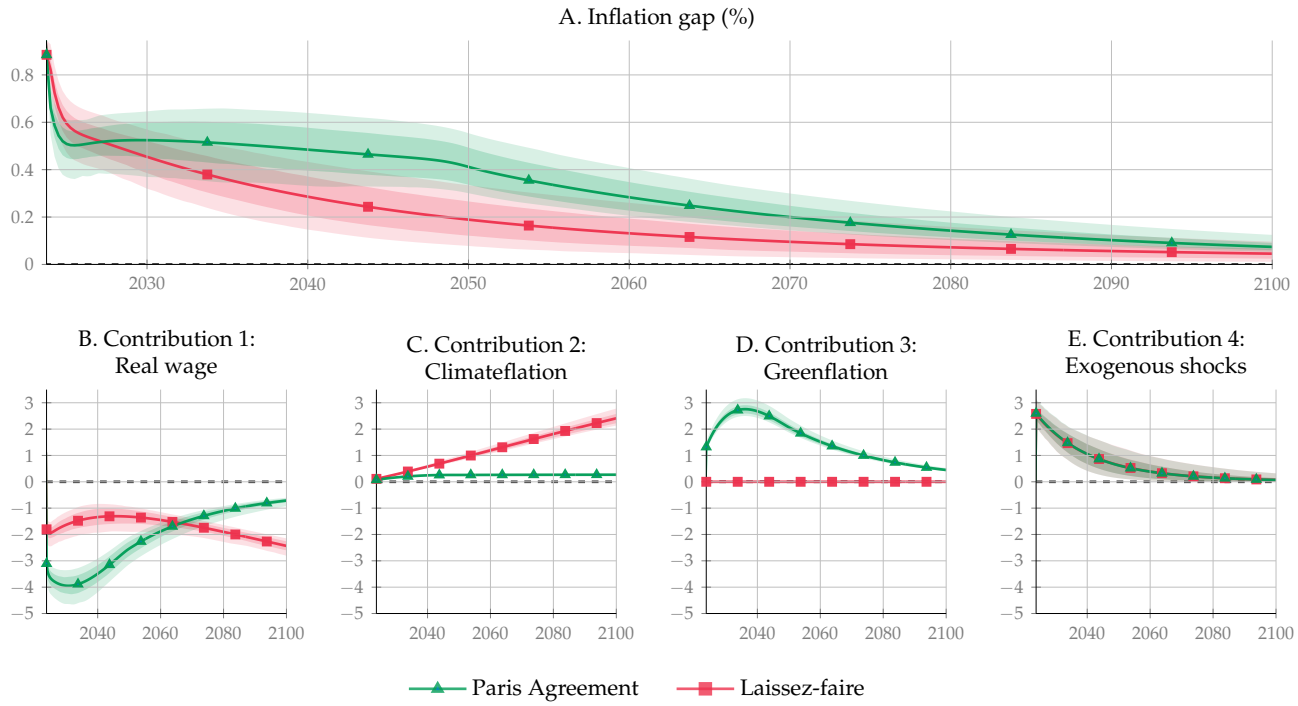
Figure 6 depicts the component-wise contributions to the inflation gap. The sum of Panels B-E corresponds to the aggregate gap in Panel A. Overall, the dynamics of the inflation gap are broadly similar across scenarios, largely reflecting a disinflationary process driven by the dissipation of previously estimated positive cost-push shock (Panel E). However, as discussed earlier, inflation remains notably more persistent under the Paris Agreement scenario. By 2050, the inflation rate is approximately 0.22 percentage points higher (or 0.88 percentage points on an annualized basis) than under the laissez-faire scenario. This quantitative estimate of greenflation aligns closely with the findings of the large-scale model of Coenen et al. (2024), though it is significantly higher than the estimates reported in Olovsson and Vestin (2023).

How can we explain this persistent increase in inflation? The decomposition under the Paris Agreement scenario reveals important differences across channels. The most exogenous source is the carbon tax, whose increase, together with associated abatement expenditures,

[30] The Shapley decomposition attributes the effect of each force (e.g., carbon taxation, climate damages, markup shocks) by averaging over all possible combinations in which variables enter the marginal cost function. Cross-product terms are shared equally among the factors, ensuring that results are independent of ordering. In linear settings, this method reduces to the standard contribution analysis, offering a natural extension to nonlinear models. It thus provides a consistent measure of how each nonlinear force contributes to inflation dynamics.

[31] To simplify the exposition, we incorporate the cost-push shock directly into marginal cost.

FIGURE 6. Decomposition of inflation during the green transition



Note: This figure reports the projected paths of the main variables in the New Keynesian climate model under two scenarios: *(i)* the Paris Agreement, with a carbon tax consistent with achieving net zero emissions by 2050, and *(ii)* laissez-faire, with no carbon tax. Shaded areas denote the uncertainty bands associated with the Paris Agreement (green) and laissez-faire (red) scenarios, obtained from 500 random draws generated using the Metropolis-Hastings sampler.

generates a strong greenflation contribution, peaking at over 3 percentage points around 2030 (panel D). In contrast, the contribution of climateflation, stemming from the productivity-reducing effects of global warming, is smaller than in the baseline and stabilizes at around 1 percentage point toward the end of the century (Panel C). The most endogenous channel is the wage contribution, which operates as a general equilibrium feedback mechanism within the model. Higher carbon taxes are inflationary, and through the Taylor principle, they induce an increase in real interest rates that crowds out consumption. The resulting wealth effect increases labor supply and pushes down real wages. Wages are therefore central in shaping how ex ante greenflation pressures translate into effective inflation: while the decline in real wages partially offsets inflationary forces, the adjustment is insufficient to neutralize them, leaving the Paris Agreement scenario more inflationary overall.

In contrast, under the laissez-faire scenario, the contribution of climateflation rises steadily relative to the baseline, exceeding 3 percentage points by the end of the century as climate-induced productivity losses accumulate (Panel C). This inflationary effect is largely offset by the negligible role of greenflation, which remains close to zero throughout (Panel B). Real wages initially decline less under laissez-faire, but over time they become increasingly eroded

by the persistent productivity deterioration caused by unchecked global warming (Panel D). Importantly, the general equilibrium feedback from wage dynamics helps partially mitigate the impact of climateflation. In the robustness analysis, we further investigate how this wage adjustment mechanism evolves under alternative degrees of wage stickiness.

In summary, our framework highlights a key result: stronger mitigation policies tend to be more inflationary, as the inflationary effects of greenflation outweigh the disinflationary effects from reduced climate damages (climateflation).[32] The overall inflationary trajectory is therefore highly sensitive to how effectively real wages adjust, which determines the extent to which climate- and policy-induced cost pressures are absorbed. In the final section, we investigate how general equilibrium mechanisms (such as the role of capital in production, wage rigidity, and the redistribution of carbon tax revenues) shape this wage adjustment and, in turn, the inflationary response.

6. Climate change and monetary policy

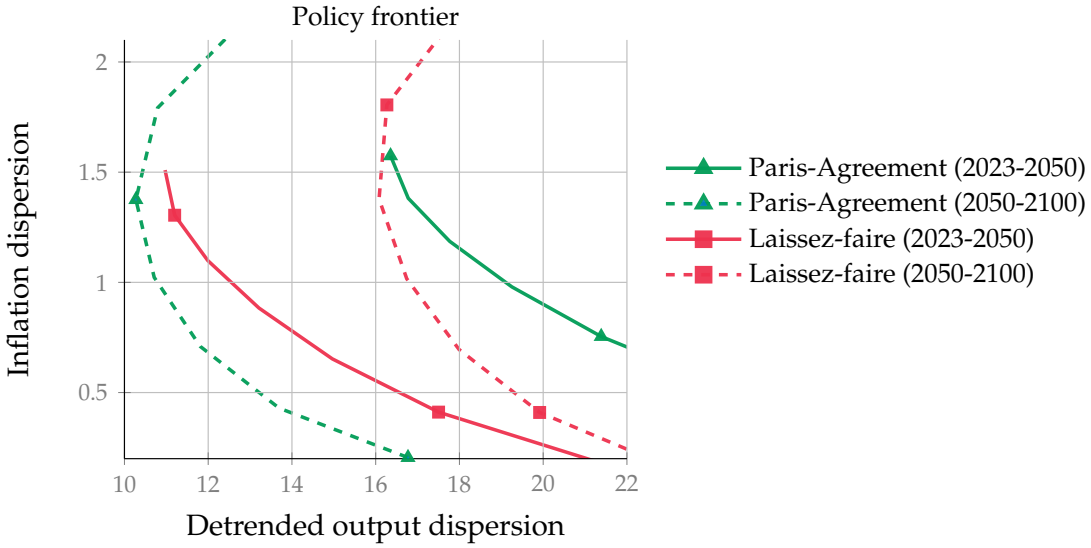
This section explores the interaction between climate change and monetary policy, building on the extensive discussion in Schnabel (2022). In particular, it examines how the central bank's inflation-output trade-off is reshaped by the structural changes induced by climate change and related mitigation policies. The section also analyzes how the design of the monetary policy rule influences the broader macroeconomic effects of climate-related shocks and policy interventions.

6.1. **Managing the inflation/output tradeoffs in the presence of climate change.**

Figure 7 illustrates how climate change and mitigation policies influence the central bank's trade-off between inflation and output stabilization. The figure plots the inflation-output variability frontier across two distinct time horizons and for two transition scenarios: (*Paris Agreement* and *laissez faire*). The first horizon corresponds to the medium run, defined as the transition period from 2023 to 2050, while the second captures the long run, covering the post-transition period from 2050 to 2100.

[32] Appendix F in the Online Appendix presents a sensitivity analysis assessing how structural parameters influence inflation, output, and interest rates during the green transition. Specifically, we examine the effects of variations in the degree of discounting, the monetary policy reaction coefficients, the slopes of the aggregate demand and Phillips curves and key climate-related parameters. The results show that greenflation intensifies when: *(i)* households are less forward-looking; *(ii)* price setters are more forward-looking; *(iii)* the central bank responds weakly to the inflation gap or strongly to the output gap; *(iv)* the Phillips curve is steeper; and *(v)* the interest elasticity of consumption is lower. Higher abatement costs also amplify inflationary pressures, whereas greater climate damages mainly reduce long-run productivity with limited effects on transition-related inflation.

FIGURE 7. Inflation-output variability frontier under alternative output gap weight in the Taylor rule



Note: This figure plots the dispersion of inflation (y-axis) against the dispersion of detrended output (x-axis) for varying values of the monetary policy response coefficient ϕ_y, under two scenarios: *(i)* the Paris Agreement (green) and *(ii)* laissez-faire (red). Inflation dispersion is measured as $\mathbb{E}\{(\pi_t - \pi_t^\star)^2\}$, while output dispersion is measured as $\mathbb{E}\{(\tilde{y}_t - \tilde{y})^2\}$. These dispersion metrics are computed by sampling shocks over 50 independent Monte Carlo chains. For each chain, the average squared deviation is calculated over a specified period (e.g., 2023Q1–2050Q2) and all 50 draws.

During the transition period, the Paris Agreement scenario shifts the inflation-output variability frontier outward and to the right relative to the laissez-faire scenario, indicating a deterioration in the trade-off between inflation and output stabilization. Depending on its loss function, the central bank may choose to contain inflation volatility at the expense of greater output variability, or vice versa, but it cannot avoid the overall worsening of the trade-off during this period. This finding is consistent with Del Negro et al. (2023), who identify similar dynamics in a multi-sector model, and resonates with the observations of Schnabel (2022), who emphasize the supply-driven nature of the greenflation shock.

Importantly, the medium-term stabilization costs of climate mitigation are offset by a significantly improved monetary policy trade-off in the long run. Between 2050 and 2100, the inflation-output variability frontier under the Paris Agreement shifts inward, indicating enhanced macroeconomic stability. Mitigation efforts thus entail short-term costs, most visibly in the form of higher inflation volatility during the transition, but they also lay the groundwork for a more stable macroeconomic environment in the second half of the century. By contrast, the laissez-faire path looks more favorable in the medium term, with lower volatility levels. Yet the absence of climate policy ultimately carries a high price of inaction: the

compounding effects of climate damages lead to substantially greater inflation and output dispersion in the long run.

6.2. **Natural rates and the design of the monetary policy rule.** As discussed in subsection 5.1, climate change and associated mitigation policies can significantly influence both the level and growth rate of natural output, as well as the natural short-term real interest rate $r^\star$, that is, the equilibrium real interest rate in an economy without nominal frictions. Monetary policy rules typically rely on constant benchmarks, such as steady-state policy rate (or inflation target), as in standard DSGE models like Smets and Wouters (2007). However, when structural forces like climate change or transition policies induce persistent shifts in the natural rate of interest, relying on this assumption can lead to systematic policy errors. As emphasized by Orphanides (2002), misperceiving the natural rate can severely impair a central bank's ability to stabilize inflation and output. In what follows, we examine how this misjudgment may undermine monetary policy effectiveness, particularly during the transition to a low-carbon economy.

To this end, we specify the monetary policy rule as a general function of the pair $(\varsigma_{r,t}, \varsigma_{y,t})$, defined as:

$$\varsigma_{r,t} = \varsigma_{r,t-1}^{\phi_r} \left[\left(\frac{\pi_t^\star}{\pi} \right) \left(\frac{\pi_t}{\pi_t^\star} \right)^{\phi_\pi} \varsigma_{y,t}^{\phi_y} \right]^{1-\phi_r} \varepsilon_{r,t}. \tag{36}$$

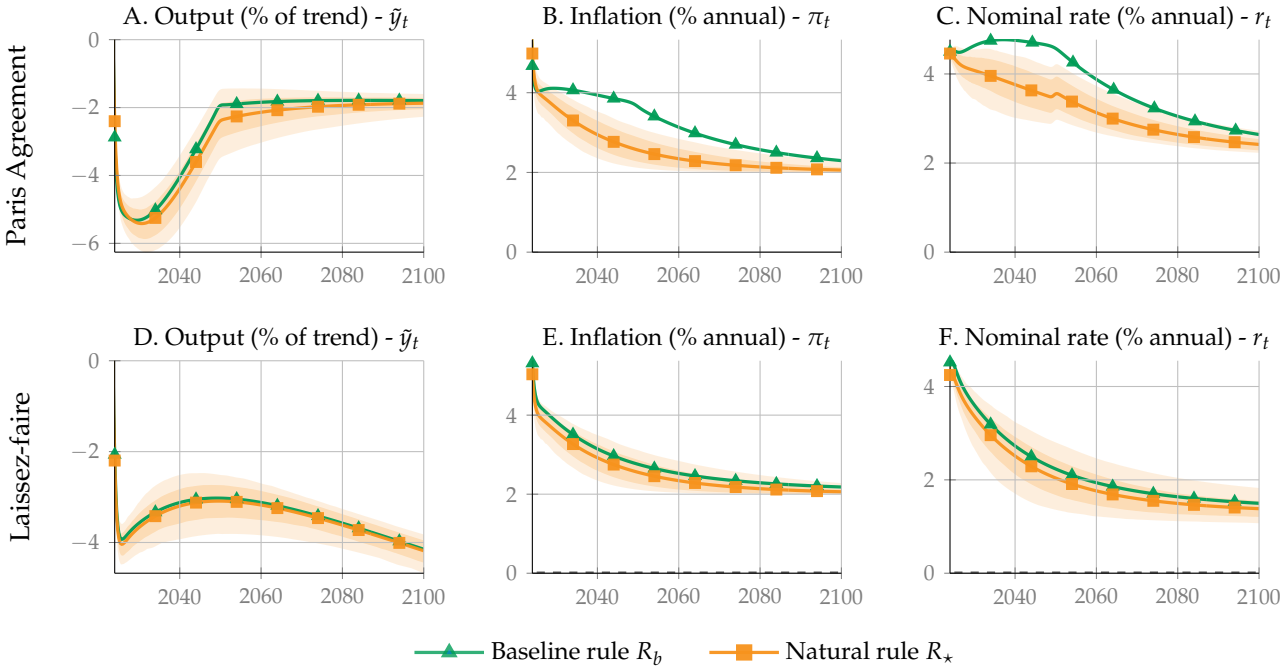
We consider two alternative specifications of this rule. The first, denoted R_b, represents the estimated baseline rule and aligns with standard formulations in macroeconomic models (e.g. Smets and Wouters, 2007). It is defined as follows:

$$(\varsigma_{r,t}, \varsigma_{y,t}) = \left(\frac{r_t}{r}, \frac{\tilde{y}_t}{\tilde{y}_t^\star} \right). \tag{37}$$

Here, the nominal interest rate is expressed relative to a constant long-run level, while output is measured against its time-varying natural counterpart, which reflects structural changes arising from climate damages as well as from the implementation of carbon taxes. However, as explained above, this approach may inadvertently imply a return to a steady-state interest rate, even in the presence of structural changes driven by climate impacts of policy interventions.

Given that the same structural forces driving natural output also influence the natural interest rate (Laubach and Williams, 2003, Holston et al., 2017), anchoring monetary policy to

FIGURE 8. The impact of climate transition under alternative monetary policy rules



Note: This figure presents the trajectories of key variables under the Paris Agreement scenario for three different monetary policy rules: *(i)* the estimated policy rule (green line), where $(\varsigma_{r,t}, \varsigma_{y,t}) = (r_t/r, \tilde{y}_t/\tilde{y}_t^\star)$, and *(ii)* a natural-rate-adjusted rule (orange line), where $(\varsigma_{r,t}, \varsigma_{y,t}) = (r_t/(r_t^\star \pi_t^\star), \tilde{y}_t/\tilde{y}_t^\star)$. The light orange area denotes the uncertainty band associated with the natural-rate-adjusted rule, derived from 500 random draws generated via the Metropolis-Hastings sampler.

a fixed long-run interest rate becomes problematic amid evolving conditions. As an alternative, we define the policy rule in terms of deviations from the time-varying natural interest rate. This specification, denoted $R_\star$, is given by:

$$(\varsigma_{r,t}, \varsigma_{y,t}) = \left(\frac{r_t}{r_t^\star \pi_t^\star}, \frac{\tilde{y}_t}{\tilde{y}_t^\star} \right). \tag{38}$$

Figure 8 illustrates the macroeconomic outcomes under both monetary policy rules. The rule that responds to both the natural output level and the natural real interest rate proves most effective in stabilizing inflation. Under both climate scenarios, it promotes a quicker convergence of inflation toward the 2% target, with only a modest increase in output volatility. By aligning policy with evolving natural rates, the central bank strengthens its capacity to stabilize the economy in the face of structural transformations induced by climate dynamics and mitigation measures.

Conversely, when the policy framework disregards the effects of climate change and mitigation policies on natural output and interest rates, inflation remains persistently above target across the projection horizon. This issue is particularly pronounced under the Paris Agreement scenario, where structural shifts are stronger. In this context, inflation exceeds

the level prevailing under the natural policy rule by 0.8 percentage points until 2050 and 0.6 until 2100. However, even under the laissez-faire scenario, failing to account for the gradual decline in productivity due to climate damages results in higher inflation. These findings underscore the imperative of adapting monetary policy frameworks to an evolving macroeconomic environment shaped by climate change.

7. Robustness analysis

In this final section, we conduct four additional exercises to test the robustness of our main findings. Specifically, we: *(i)* introduce sticky wages alongside sticky prices to capture broader nominal rigidities; *(ii)* modify the redistribution scheme for carbon tax revenues to evaluate alternative fiscal policies; *(iii)* model abatement as a durable good; and *(iv)* incorporate capital accumulation into the production function to reflect investment dynamics. These extensions leave the underlying drivers of greenflation and climateflation unchanged from our baseline (*Paris Agreement*) analysis, as they do not alter the structural channels through which carbon taxes and climate damages exert pressure on marginal costs. However, they do affect the general equilibrium adjustment of the economy which in turn shapes how these inflationary forces materialize ex post.

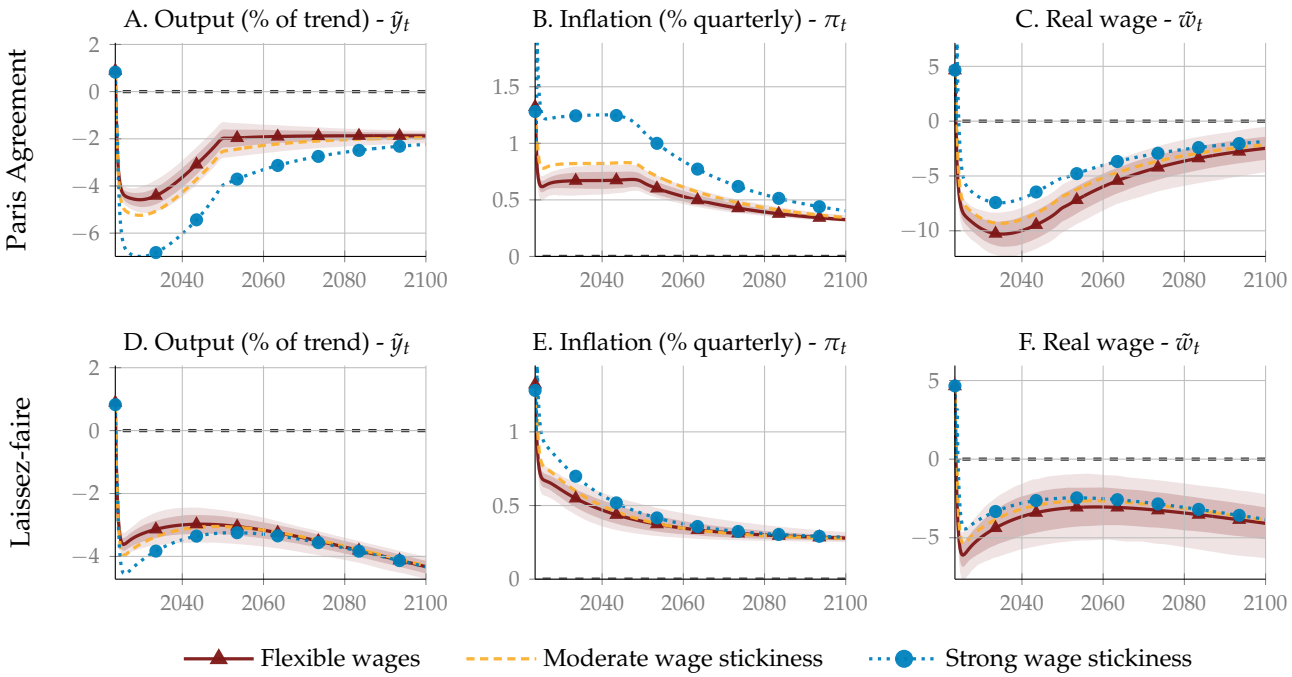
7.1. **Sticky wages.** The inflation decomposition in subsection 5.3 reveals that real wages adjust rapidly in response to climate-induced damages. To examine whether wage rigidity amplifies the impact of climate shocks, particularly the phenomenon of greenflation, on realized inflation, we introduce nominal wage stickiness into the model. Specifically, we assume that: *(i)* the labor market exhibits monopolistic competition; *(ii)* households delegate wage-setting decisions to employment agencies, following the framework of Erceg et al. (2000); and *(iii)* there are quadratic adjustment costs associated with changes in individual nominal wages $W_{i,t}$ for $i \in [0, l_t]$:

$$\mathcal{C}^w_{i,t} = \frac{\kappa_w}{2}\left(\frac{W_{i,t}}{W_{i,t-1}} - \pi^\star_t\right)^2 \frac{W_{i,t}}{P_t} n^s_{i,t}, \tag{39}$$

where $\kappa_w > 0$ denotes the wage stickiness parameter.[33]

[33]Each household supplies a differentiated type of labor $n_{i,t}$ monopolistically. At each time t, a continuum of perfectly competitive "employment agencies" aggregates this specialized labor into a homogeneous labor input n^d_t, which is sold to firms according to the CES aggregator: $n^d_t = (\int_0^1 n_{i,t}^{(\zeta_w-1)/\zeta_w}\,\mathrm{d}i)^{\zeta_w/(\zeta_w-1)}$. Profit maximization by these agencies yields the labor demand for type-i labor as $n_{i,t} = (W_{i,t}/W_t)^{-\zeta_w} n^d_t$, where $W_t = \left(\int_0^1 W_{i,t}^{1-\zeta_w}, \mathrm{d}i\right)^{1/(1-\zeta_w)}$ is the aggregate nominal wage index. The parameter ζ_w denotes the elasticity of substitution between different labor types.

FIGURE 9. The role of wage stickiness



Note: The light red area denotes the uncertainty band under the flexible-wage assumption, based on 500 random draws generated using the Metropolis-Hastings sampler. The detrended real wage is defined as $\tilde{w}_t = w_t/z_t$. Since all simulations incorporate the effects of the wage markup, the flexible-wage path does not exactly coincide with the baseline results reported earlier in the paper.

Figure 9 displays the trajectories of key macroeconomic variables under both the Paris Agreement scenario (top row) and the laissez-faire scenario (bottom row), for varying degrees of wage stickiness. In addition to the baseline case with flexible wages, we consider two alternative degrees of nominal wage rigidity: moderate rigidity with $\kappa_w = 10$ and pronounced rigidity with $\kappa_w = 20$. The results show that wage stickiness amplifies the inflationary response to climate shocks and leads to a more pronounced economic contraction. This occurs because slower real wage adjustment prevents households from fully absorbing the rise in firms' marginal costs associated with climate damages and carbon taxes. Consequently, the inflationary pressures from both climateflation and greenflation become more persistent, while the output gap widens. These findings are consistent with those of Olovsson and Vestin (2023) and Del Negro et al. (2023), who also report that nominal wage rigidity increases inflation during the energy transition in dynamic general equilibrium models.

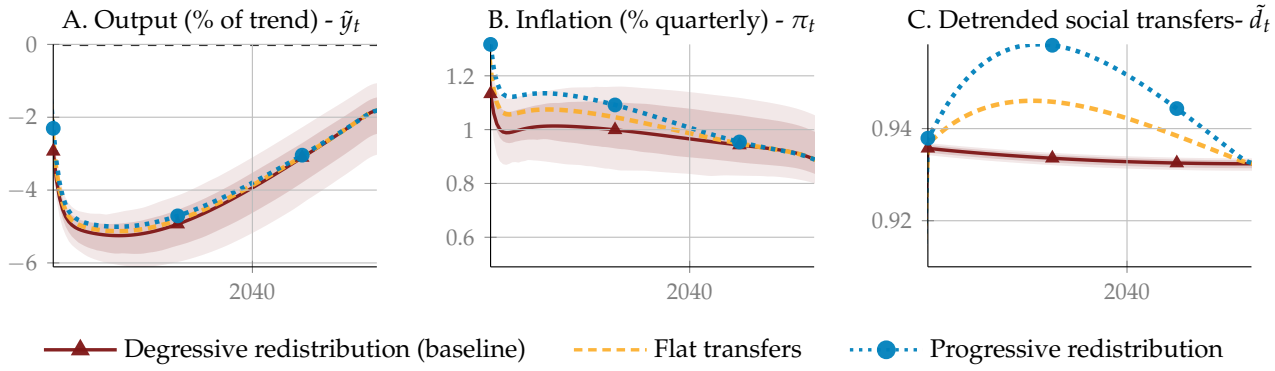
7.2. **Redistribution of carbon tax revenues.** In the baseline scenario, carbon tax revenues are fully redistributed to Ricardian households for simplicity. In this setting, the transfers have a negligible effect on aggregate consumption, as Ricardian households are forward-looking and adjust their behavior primarily in response to changes in distorting taxes and interest

rates, not lump-sum transfers. However, alternative redistribution schemes can be explored by generalizing the transfer rule as:

$$d_{i,t} = z_t l_t \Phi\left(m_t\right) d + v \frac{T^e_{i,t}}{\omega}, \tag{40}$$

where $v \in [0,1]$ governs the share of carbon tax revenues redistributed to low-productivity households. The baseline case, denoted as "regressive redistribution", assumes $v = 0.$, meaning all transfers go to Ricardian households. Alternatively, a "flat transfer" scheme sets $v = 1/2$, under which both household types receive equal transfers. Finally, a "progressive redistribution" scheme is represented by $v = 2/3$, implying that low-productivity households receive twice as much as high-productivity households.

FIGURE 10. The role of social transfers during the transition

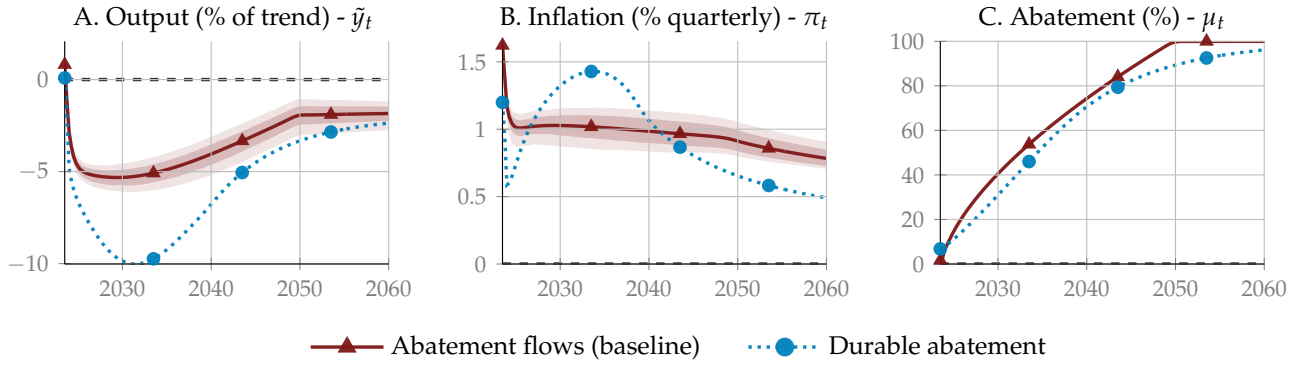


Note: The light red area denotes the uncertainty band under degressive redistribution (baseline) assumption, based on 500 random draws generated using the Metropolis-Hastings sampler.

Figure 10 illustrates the macroeconomic effects of these three redistribution schemes under the Paris Agreement scenario. Flat or progressive redistribution channels additional income to households with a high marginal propensity to consume. These households spend most or all of their transfers, thereby raising aggregate demand. The resulting demand effect modestly increases GDP and consumption, but also generates higher inflationary pressures. These findings are consistent with heterogeneous-agent models such as Benmir and Roman (2022), Langot et al. (2023), and Auclert et al. (2023), which emphasize the importance of redistribution mechanisms in shielding vulnerable households from the inflationary effects of carbon tax policies. Our two-type agent framework, though stylized, successfully reproduces results typically obtained only in full-fledged heterogeneous-agent models, demonstrating that even simple redistribution rules can materially influence inflation dynamics.

7.3. **Abatement as investment goods.** In standard DICE models, abatement is modeled as a flow variable that can adjust instantly and without cost in response to changes in the carbon tax. In reality, however, many abatement measures involve durable investments, such as infrastructure, that are costly and not easily reversible. To reflect this, we modify Equation (9) to: $\mathcal{C}^a_{j,t} = \theta_{1,t}\Im^{\theta_2}_{j,t} y_{j,t}$, where $\Im_{j,t}$ denotes the flow of new durable abatement goods. The stock of abatement capital evolves according to $\mu_{j,t} = (1-\delta_\mu)\mu_{j,t-1} + \Im_{j,t}$, with $\delta_\mu = 0.025$, implying a 40-year average lifetime, consistent with infrastructure investment. In the DICE framework, cumulative abatement spending under the Paris Agreement scenario amount to 71% of 2020 GDP. We calibrate the cost parameter $\theta_{1,2020}$ up to 1,050 to match this benchmark.

FIGURE 11. Transition dynamics with durable abatement investments



Note: The light red area denotes the uncertainty band under the abatement-flows (baseline) assumption, based on 500 random draws generated using the Metropolis-Hastings sampler.

Figure 11 illustrates the transition dynamics under the Paris Agreement scenario, comparing two assumptions about the lifetime of abatement goods. The red curve depicts the baseline case, where abatement goods are non-durable and expire after one period. In contrast, the blue dotted curve shows the scenario with durable abatement goods, where investments accumulate and persist over time. The results indicate that durability substantially increases the initial transition cost: achieving net-zero emissions requires large upfront investments with limited scope to defer expenditures. As a result, GDP declines by up to 10% in 2035, and inflationary pressures remain stronger than in the non-durable baseline until the transition is completed. Once net zero is achieved, however, durability no longer generates additional inflationary pressures.

7.4. **Capital in the production function.** Thus far, we have simplified the production side of the economy by considering labor as the sole input. This assumption facilitated the derivation of a tractable system of equations in the spirit of Woodford (2003). However, in integrated

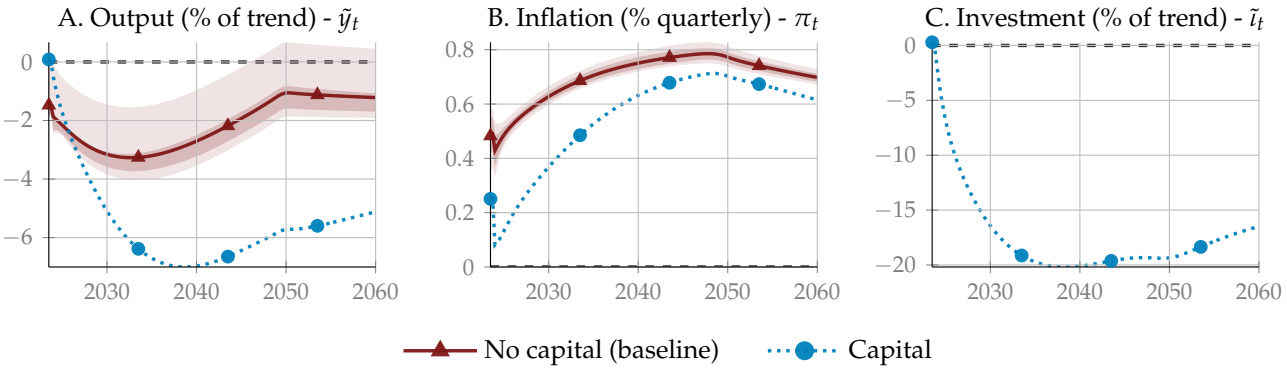
assessment models such as DICE, capital plays a more prominent role in determining output and long-run growth. In this section, we explore whether and how the inclusion of capital affects the dynamics of the green transition.

To this end, we extend the production function of firm j to incorporate capital $k_{j,t}$ as follows:

$$y_{j,t} = \Phi(m_t) \left(z_t n_{j,t}^d \right)^{\alpha} k_{j,t-1}^{1-\alpha}. \tag{41}$$

where $\alpha = 0.7$ denotes the labor share in the production function. The accumulation of capital is given by $k_{j,t} = (1-\delta) k_{j,t-1} + \left(1 - \mathcal{C}_{j,t}^{\iota}\right) \iota_{j,t}$, where δ is the capital depreciation rate, $\iota_{j,t}$ is investment and $\mathcal{C}_{j,t}^{\iota}$ are investment adjustment costs. These costs are given by $\mathcal{C}_{j,t}^{\iota} = \frac{\kappa_\iota}{2} \left(\frac{\iota_{j,t}}{\iota_{j,t-1}} - g_{z,t} \right)^2$, with κ_ι being a parameter that determines the magnitude of the costs.

FIGURE 12. The role of capital in the production function during the transition



Note: The light red area denotes the uncertainty band under the no-capital (baseline) assumption, based on 500 random draws generated using the Metropolis-Hastings sampler. Detrended investment is defined as $\tilde{\iota}_t = \iota_t / (l_t z_t)$. For comparability, estimated shocks are omitted here, as in the capital-augmented model they would build up and propagate through the capital stock, producing larger deviations. For this reason, the no-capital case shown here does not exactly correspond to the baseline simulations reported earlier in the paper.

Figure 12 illustrates the trajectory of the economy under the Paris Agreement scenario, comparing outcomes with and without capital. For comparability, no estimated shocks are introduced into the simulations, so that differences reflect only the role of capital accumulation. In the extended model with capital, the depreciation rate is set to $\delta = 0.015$ and the investment adjustment cost parameter to $\kappa_\iota = 1$. The inclusion of capital reveals that the green transition induces a pronounced crowding-out of conventional investment. Rising abatement spending reduces firms' profits and lowers their incentives to invest. The resulting decline in investment dampens aggregate demand and, consequently, inflation. These dynamics imply that allowing for capital accumulation deepens the recession while lowering marginal production costs, thereby attenuating inflationary pressures relative to the baseline model.

8. Conclusion

This paper develops and estimates a nonlinear New Keynesian Climate (NKC) model that integrates the long-term dynamics of climate change with the nominal frictions central to monetary policy. By bridging the gap between Integrated Assessment Models and modern DSGE frameworks, the NKC model provides a unified and tractable environment to analyze the macroeconomic and inflationary consequences of both climate damages (climateflation) and mitigation efforts (greenflation). Using Bayesian estimation on quarterly global data from 1985 to 2023, the model delivers empirically disciplined insights into how carbon pricing, nominal rigidities, and structural trends interact to shape the global economy through 2100.

Our analysis yields several key findings. First, nominal rigidities play a critical role in determining the social cost of carbon and, consequently, the optimal path of carbon pricing. Ignoring price stickiness leads to miscalibrated carbon taxes, excessive inflation, and welfare losses through reduced consumption. Second, Paris-aligned mitigation efforts are inherently inflationary in the short to medium term, as greenflation dominates climateflation. Third, these inflationary pressures entail a trade-off for central banks: accommodating the transition implies temporary deviations from inflation targets but prevents larger long-run welfare losses associated with climate damages. The results also highlight that delayed mitigation amplifies output volatility and long-term economic costs, underscoring the importance of early and credible policy action.

From a policy perspective, the findings point to the need for climate-consistent monetary frameworks. Traditional Taylor rules that ignore the structural rise in the natural rate of interest during the transition risk persistent inflation overshooting. In contrast, climate-adaptive rules that internalize shifts in equilibrium rates and the evolving inflation-output trade-off improve macroeconomic stabilization. Moreover, integrating nominal frictions into climate policy design refines the measurement of the social cost of carbon and enhances the political feasibility of ambitious mitigation pathways by minimizing inflationary side effects.

Overall, effective climate policy cannot be decoupled from sound monetary policy. Ensuring both price stability and environmental sustainability demands that central banks evolve their strategies to meet the challenges of the green transition.

References

Adjemian, S. and Juillard, M. (2014). Assessing long run risk in a DSGE model under ZLB with the stochastic extended path approach. *Mimeo*, CEPREMAP.

Adjemian, S., Juillard, M., Karamé, F., Mutschler, W., Pfeifer, J., Ratto, M., Rion, N., and Villemot, S. (2024). Dynare: Reference manual, version 6. *Dynare Working Paper #80*, CEPREMAP.

Annicchiarico, B. and Di Dio, F. (2015). Environmental policy and macroeconomic dynamics in a New Keynesian model. *Journal of Environmental Economics and Management*, 69:1–21.

Auclert, A., Monnery, H., Rognlie, M., and Straub, L. (2023). Managing an energy shock: Fiscal and monetary policy. *Working Paper #31543*, National Bureau of Economic Research.

Auer, R., Borio, C., and Filardo, A. (2017). The globalisation of inflation: The growing importance of global value chains. *Working Paper #602*, Bank for International Settlements.

Bailey, M. J. (1956). The welfare cost of inflationary finance. *Journal of Political Economy*, 64:93–110.

Baleyte, J., Bazot, G., Monnet, E., and Morys, M. (2024). High temperature shocks are supply shocks. evidence from one century of monthly data. *Discussion Paper #19682*, Centre for Economic Policy Research.

Barrage, L. (2020). Optimal dynamic carbon taxes in a climate–economy model with distortionary fiscal policy. *The Review of Economic Studies*, 87:1–39.

Barrage, L. and Nordhaus, W. (2024). Policies, projections, and the social cost of carbon: Results from the dice-2023 model. *Proceedings of the National Academy of Sciences*, 121:e2312030121.

Benigno, P. and Eggertsson, G. B. (2023). It's baaack: The surge in inflation in the 2020s and the return of the non-linear Phillips curve. *Working Paper #31197*, National Bureau of Economic Research.

Benmir, G. and Roman, J. (2022). The distributional costs of net-zero: A hank perspective. *Mimeo*, London School of Economics.

Bilal, A. and Känzig, D. R. (2024). The macroeconomic impact of climate change: Global vs. local temperature. *Working Paper #32450*, National Bureau of Economic Research.

Bilal, A. and Känzig, D. R. (2025). Does unilateral decarbonization pay for itself? *AEA Papers and Proceedings*, 115:369–373.

Bilbiie, F., Ghironi, F., and Melitz, M. (2012). Endogenous entry, product variety, and business cycles. *Journal of Political Economy*, 120:304–345.

Cai, Y. and Lontzek, T. (2019). The social cost of carbon with economic and climate risks. *Journal of Political Economy*, 127:2684–2734.

Chow, G. C. and Lin, A.-L. (1971). Best linear unbiased interpolation, distribution, and extrapolation of time series by related series. *The Review of Economics and Statistics*, 53:372–375.

Christiano, L., Motto, R., and Rostagno, M. (2014). Risk shocks. *American Economic Review*, 104:27–65.

Clarida, R., Gali, J., and Gertler, M. (1999). The science of monetary policy: a new keynesian perspective. *Journal of Economic Literature*, 37:1661–1707.

Cochrane, J. H. (2001). Long-term debt and optimal policy in the fiscal theory of the price level. *Econometrica*, 69:69–116.

Coenen, G., Lozej, M., and Priftis, R. (2024). Macroeconomic effects of carbon transition policies: an assessment based on the ECB's new area-wide model with a disaggregated energy sector. *European Economic Review*, 167:104798.

Cuba-Borda, P., Guerrieri, L., Iacoviello, M., and Zhong, M. (2019). Likelihood evaluation of models with occasionally binding constraints. *Journal of Applied Econometrics*, 34:1073–1085.

Dechezleprêtre, A., Fabre, A., Kruse, T., Planterose, B., Sanchez Chico, A., and Stantcheva, S. (2025). Fighting climate change: International attitudes toward climate policies. *American Economic Review*, 115:1258–1300.

Del Negro, M., di Giovanni, J., and Dogra, K. (2023). Is the green transition inflationary? *Staff Reports #1053*, Federal Reserve Bank of New York.

Del Negro, M., Giannoni, M. P., and Patterson, C. (2023). The forward guidance puzzle. *Journal of Political Economy Macroeconomics*, 1:43–79.

Del Negro, M., Giannoni, M. P., and Schorfheide, F. (2015). Inflation in the great recession and new keynesian models. *American Economic Journal: Macroeconomics*, 7:168–196.

Di Tella, R., MacCulloch, R. J., and Oswald, A. J. (2001). Preferences over inflation and unemployment: Evidence from surveys of happiness. *American Economic Review*, 91:335–341.

Dietz, S., van Der Ploeg, F., Rezai, A., and Venmans, F. (2021). Are economists getting climate dynamics right and does it matter? *Journal of the Association of Environmental and Resource Economists*, 8:895–921.

Erceg, C. J., Henderson, D. W., and Levin, A. T. (2000). Optimal monetary policy with staggered wage and price contracts. *Journal of Monetary Economics*, 46:281–313.

Fair, R. and Taylor, J. (1983). Solution and maximum likelihood estimation of dynamic nonlinear rational expectations models. *Econometrica*, 51:1169–1185.

Fernández-Villaverde, J., Gillingham, K., and Scheidegger, S. (2025). Climate change through the lens of macroeconomic modeling. *Annual Review of Economics*, Forthcoming.

Fernández-Villaverde, J., Rubio-Ramírez, J. F., and Schorfheide, F. (2016). Solution and estimation methods for DSGE models. In *Handbook of Macroeconomics*, volume 2, pages 527–724. Elsevier.

Fève, P., Matheron, J., and Sahuc, J.-G. (2010). Inflation target shocks and monetary policy inertia in the euro area. *The Economic Journal*, 120:1100–1124.

Finkelstein Shapiro, A. and Metcalf, G. E. (2023). The macroeconomic effects of a carbon tax to meet the US Paris Agreement target: The role of firm creation and technology adoption. *Journal of Public Economics*, 218:104800.

Folini, D., Friedl, A., Kübler, F., and Scheidegger, S. (2025). The climate in climate economics. *Review of Economic Studies*, 92:299–338.

Fornaro, L., Guerrieri, V., and Reichlin, L. (2025). Monetary policy for the green transition. *Mimeo*, Centre de Recerca en Economia Internacional.

Fried, S. (2022). Seawalls and stilts: A quantitative macro study of climate adaptation. *The Review of Economic Studies*, 89:3303–3344.

Gabaix, X. (2020). A behavioral new keynesian model. *American Economic Review*, 110:2271–2327.

Galí, J. (2008). *Monetary policy, inflation, and the business cycle*. Princeton University Press.

Golosov, M., Hassler, J., Krusell, P., and Tsyvinski, A. (2014). Optimal taxes on fossil fuel in general equilibrium. *Econometrica*, 82:41–88.

Guerrieri, L. and Iacoviello, M. (2017). Collateral constraints and macroeconomic asymmetries. *Journal of Monetary Economics*, 90:28–49.

Harding, M., Lindé, J., and Trabandt, M. (2023). Understanding post-covid inflation dynamics. *Journal of Monetary Economics*, 140:S101–S118.

Hazell, J., Herreno, J., Nakamura, E., and Steinsson, J. (2022). The slope of the phillips curve: evidence from us states. *The Quarterly Journal of Economics*, 137:1299–1344.

Holston, K., Laubach, T., and Williams, J. C. (2017). Measuring the natural rate of interest: International trends and determinants. *Journal of International Economics*, 108:S59–S75.

IPCC (2021). Climate change 2021: The physical science basis: summary for policymakers. Contribution of Working Group I to the Sixth Assessment Report of the Intergovernmental Panel on Climate Change.

Ireland, P. N. (2007). Changes in the federal reserve's inflation target: Causes and consequences. *Journal of Money, Credit and Banking*, 39:1851–1882.

Jensen, S. and Traeger, C. P. (2014). Optimal climate change mitigation under long-term growth uncertainty: Stochastic integrated assessment and analytic findings. *European Economic Review*, 69:104–125.

Jiang, Z. and Richmond, R. J. (2024). Reserve asset competition and the global fiscal cycle. NBER Working Papers #*32841*, National Bureau of Economic Research.

Jo, A. and Miftakhova, A. (2024). How constant is constant elasticity of substitution? Endogenous substitution between clean and dirty energy. *Journal of Environmental Economics and Management*, 125:102982.

Jondeau, E., Levieuge, G., Sahuc, J.-G., and Vermandel, G. (2025). Environmental subsidies to mitigate net-zero transition costs. *American Economic Journal: Macroeconomics*, Forthcoming.

Juillard, M. (1996). Dynare: A program for the resolution and simulation of dynamic models with forward variables through the use of a relaxation algorithm. *Working Paper #9602*, CEPREMAP.

Känzig, D. R. (2023). The unequal economic consequences of carbon pricing. *Working Paper #31221*, National Bureau of Economic Research.

Känzig, D. R. and Konradt, M. (2024). Climate policy and the economy: Evidence from europe's carbon pricing initiatives. *IMF Economic Review*, 72:1081–1124.

Langot, F., Malmberg, S., Tripier, F., and Hairault, J.-O. (2023). The macroeconomic and redistributive effects of shielding consumers from rising energy prices: A real time evaluation of the french experiment. *Working Paper #2305*, CEPREMAP.

Laubach, T. and Williams, J. C. (2003). Measuring the natural rate of interest. *Review of Economics and Statistics*, 85:1063–1070.

Leeper, E. M. (1991). Equilibria under 'active' and 'passive' monetary and fiscal policies. *Journal of Monetary Economics*, 27:129–147.

Lucas, Jr, R. E. (2000). Inflation and welfare. *Econometrica*, 68:247–274.

McKay, A., Nakamura, E., and Steinsson, J. (2016). The power of forward guidance revisited. *American Economic Review*, 106:3133–3158.

McKay, A., Nakamura, E., and Steinsson, J. (2017). The discounted Euler equation: A note. *Economica*, 84:820–831.

Nakamura, E., Steinsson, J., Sun, P., and Villar, D. (2018). The elusive costs of inflation: Price dispersion during the u.s. great inflation. *The Quarterly Journal of Economics*, 133:1933–1980.

Nakov, A. and Thomas, C. (2023). Climate-conscious monetary policy. *Working Paper #2845*, European Central Bank.

Nordhaus, W. (1992). The 'DICE' model: Background and structure of a dynamic integrated climate-economy model of the economics of global warming. *Technical Report*, Cowles Foundation for Research in Economics, Yale University.

Nordhaus, W. D. (2017). Revisiting the social cost of carbon. *Proceedings of the National Academy of Sciences*, 114:1518–1523.

Nuño, G., Renner, P., and Scheidegger, S. (2024). Monetary policy with persistent supply shocks. *Working Paper #11463*, CESifo.

OECD (2017). Entrepreneurship at a Glance. *OECD Publishing*.

Olovsson, C. and Vestin, D. (2023). Greenflation? *Working Paper #420*, Sveriges Riksbank.

Orphanides, A. (2002). Monetary-policy rules and the great inflation. *American economic review*, 92:115–120.

Pappa, E., Airaudo, F., and Seoane, H. D. (2023). The green metamorphosis of a small open economy. *Discussion Paper #17863*, Centre for Economic Policy Research.

Pindyck, R. (2013). Climate Change Policy: What do the models tell us? *Journal of Economic Literature*, 51:860–872.

Rey, H. (2015). Dilemma not trilemma: The global financial cycle and monetary policy independence. *Working Paper #21162*, National Bureau of Economic Research.

Schnabel, I. (2022). A new age of energy inflation: climateflation, fossilflation and greenflation. In *Remarks at a panel on Monetary Policy and Climate Change at The ECB and its Watchers XXII Conference, Frankfurt am Main*, volume 17.

Shiller, R. J. (1997). Why do people dislike inflation? In *Reducing inflation: Motivation and strategy*, pages 13–70. University of Chicago Press.

Smets, F. and Wouters, R. (2007). Shocks and frictions in US business cycles: A Bayesian DSGE approach. *American Economic Review*, 97:586–606.

van den Bremer, T. S. and van der Ploeg, F. (2021). The risk-adjusted carbon price. *American Economic Review*, 111:2782–2810.

van der Ploeg, F. and Rezai, A. (2020). The risk of policy tipping and stranded carbon assets. *Journal of Environmental Economics and Management*, 100:102258.

Woodford, M. (1995). Price-level determinacy without control of a monetary aggregate. *Carnegie-Rochester Conference Series on Public Policy*, 43:1–46.

Woodford, M. (2003). *Interest and Prices: Foundations of a Theory of Monetary Policy*. Princeton University Press.

Woodford, M. (2019). Monetary policy analysis when planning horizons are finite. *NBER Macroeconomics Annual*, 33:1–50.

– Online Appendix –

Appendix A. Full model

This appendix presents the full set of equations. It includes four core equations and variables $\{\tilde{y}_t, \pi_t, r_t, m_t\}$:

$$\tilde{\lambda}_t = \beta \mathbb{E}_t \left\{ \frac{r_t}{\pi_{t+1}} \left((1-\omega)\, \tilde{\lambda}_{t+1} + \omega \varepsilon_{b,t+1} \tilde{d}_{t+1}^{-\sigma_c} \right) \right\} \tag{A.1}$$

$$(\pi_t - \pi_t^\star)\, \pi_t = (1-\vartheta)\beta \mathbb{E}_t \left\{ (1+g_{z,t+1}) \frac{\tilde{\lambda}_{t+1}}{\tilde{\lambda}_t} \frac{\tilde{y}_{t+1}}{\tilde{y}_t} \left(\pi_{t+1} - \pi_{t+1}^\star \right) \pi_{t+1} \right\} + \frac{\zeta}{\kappa} \varepsilon_{p,t} mc_t + \frac{1-\zeta}{\kappa} \tag{A.2}$$

$$\frac{r_t}{r} = \left(\frac{r_{t-1}}{r} \right)^{\phi_r} \left[\left(\frac{\pi_t^\star}{\pi} \right) \left(\frac{\pi_t}{\pi_t^\star} \right)^{\phi_\pi} \left(\frac{\tilde{y}_t}{\tilde{y}_t^\star} \right)^{\phi_y} \right]^{1-\phi_r} \varepsilon_t^r \tag{A.3}$$

$$m_t = m_{t-1} + \xi_m \sigma_t \left(1 - \tilde{\tau}_{e,t}^{\frac{1}{\theta_2 - 1}} \right) z_t l_t \tilde{y}_t \varepsilon_{e,t} \tag{A.4}$$

The model also includes auxiliary variables:

$$\tilde{\lambda}_t = \left(\frac{x_t \tilde{y}_t - \omega \tilde{d}_t}{1-\omega} \right)^{-\sigma_c} \tag{A.5}$$

$$x_t = 1 - (1-\vartheta) \frac{\kappa}{2} \left(\pi_t - \pi_t^\star \right)^2 - \theta_{1,t} \tilde{\tau}_{e,t}^{\theta_2/(\theta_2-1)} \tag{A.6}$$

$$mc_t = \frac{\psi}{(1-\omega)^{\sigma_c+\sigma_n}} \frac{\left(x_t \tilde{y}_t - \omega \tilde{d}_t \right)^{\sigma_c} \tilde{y}_t^{\sigma_n}}{\epsilon_{b,t} \Phi\left(m_t\right)^{1+\sigma_n}} + \theta_{1,t} \tilde{\tau}_{e,t} \left[\theta_2 + (1-\theta_2)\, \tilde{\tau}_{e,t}^{\frac{1}{\theta_2 - 1}} \right] \tag{A.7}$$

where $\tilde{y}_t = y_t / (z_t l_t)$, $\tilde{d}_t = d_t / z_t = d\Phi(m_t)$, and $\tilde{\tau}_{e,t} = \tau_{e,t} \sigma_t \varepsilon_{e,t} / (\theta_2 \theta_{1,t})$.

The auxiliary variable x_t is deduced from the resource constraint in Equation 22 where $l_t c_t = x_t y_t$. The aggregate marginal cost mc_t is obtained as follows. First, we know that:

$$mc_t = \frac{w_t}{\Gamma_t} + \theta_{1,t} \mu_t^{\theta_2} + \tau_{e,t} \sigma_t \left(1 - \mu_t\right) \varepsilon_{e,t}.$$

Let us consider the real wage of the high productive worker $w_t = \psi_t (n_t^s)^{\sigma_n} / \lambda_t$, the general equilibrium condition $(1-\omega)\, n_t^s = n_t^d = n_t$ and the production function $y_t = l_t \Gamma_t n_t^d$, we obtain:

$$mc_t = \frac{1}{\lambda_t \Gamma_t} \psi_t \left(\frac{y_t}{l_t \Gamma_t} \frac{1}{1-\omega} \right)^{\sigma_n} + \theta_{1,t} \mu_t^{\theta_2} + \tau_{e,t} \sigma_t \left(1 - \mu_t\right) \varepsilon_{e,t}.$$

Recall that $\Gamma_t = \Phi\left(m_t\right) z_t$ and $\tilde{y}_t = y_t / (l_t z_t)$, thus:

$$mc_t = \frac{1}{\lambda_t \Phi\left(m_t\right)} \psi z_t^{-\sigma_c} \left(\frac{\tilde{y}_t}{\Phi\left(m_t\right)} \frac{1}{1-\omega} \right)^{\sigma_n} + \theta_{1,t} \mu_t^{\theta_2} + \tau_{e,t} \sigma_t \left(1 - \mu_t\right) \varepsilon_{e,t.}$$

Next, replacing λ_t by $z_t^{-\sigma_c}\tilde{\lambda}_t$ gives:

$$mc_t = \frac{\psi}{\varepsilon_{b,t}\left(\frac{x_t\tilde{y}_t-\omega\tilde{d}_t}{1-\omega}\right)^{-\sigma_c}\Phi\left(m_t\right)}\left(\frac{\tilde{y}_t}{\Phi\left(m_t\right)}\frac{1}{1-\omega}\right)^{\sigma_n}+\tilde{\tau}_{e,t}\theta_{1,t}\left(\theta_2+\tilde{\tau}_{e,t}^{\frac{1}{\theta_2-1}}\left(1-\theta_2\right)\right),$$

$$mc_t = \frac{\psi}{\left(1-\omega\right)^{\sigma_c+\sigma_n}}\frac{\left(x_t\tilde{y}_t-\omega\tilde{d}_t\right)^{\sigma_c}\tilde{y}_t^{\sigma_n}}{\varepsilon_{b,t}\Phi\left(m_t\right)^{1+\sigma_n}}+\tilde{\tau}_{e,t}\theta_{1,t}\left(\theta_2+\tilde{\tau}_{e,t}^{\frac{1}{\theta_2-1}}\left(1-\theta_2\right)\right).$$

Finally, the model comprises five trend related deterministic processes

$$\sigma_t = \sigma_{t-1}(1-g_{\sigma,t}) \quad \text{and} \quad g_{\sigma,t} = (1-\delta_\sigma)\, g_{\sigma,t-1}, \tag{A.8}$$

$$z_t = z_{t-1}(1+g_{z,t}) \quad \text{and} \quad g_{z,t} = (1-\delta_z)\, g_{z,t-1}, \tag{A.9}$$

$$\theta_{1,t} = (p_b/\theta_2)(1-\delta_{pb})^{t-t_0}\sigma_t, \tag{A.10}$$

$$l_t = l_{t-1}\left(l_\infty/l_{t-1}\right)^{\ell_g}, \tag{A.11}$$

$$\pi_t^\star = \delta_{\pi^\star}\pi + (1-\delta_{\pi^\star})\pi_{t-1}^\star, \tag{A.12}$$

and four stochastic processes:

$$\varepsilon_{b,t} = (1-\rho_b) + \rho_b\varepsilon_{b,t-1} + \eta_{b,t}; \quad \varepsilon_{p,t} = (1-\rho_p) + \rho_p\varepsilon_{p,t-1} + \eta_{p,t}; \tag{A.13}$$

$$\varepsilon_{e,t} = (1-\rho_e) + \rho_e\varepsilon_{e,t-1} + \eta_{e,t}; \quad \varepsilon_{r,t} = (1-\rho_r) + \rho_r\varepsilon_{r,t-1} + \eta_{r,t}. \tag{A.14}$$

Appendix B. The extended path approach

A perfect foresight algorithm typically requires *(i)* a finite number of periods and *(ii)* a terminal period to compute each endogenous variable in order to realize economic surprises. To fix notation, this general representation in the presence of extended path takes the form:

$$\tilde{y}_t = g_\Theta\left(y_0, y, 0\right) \tag{B.1}$$

$$y_t = \mathbb{E}_{t,t+S}\left\{g_\Theta\left(y_{t-1}, \tilde{y}_{t+S+1}, \varepsilon_t\right)\right\} \tag{B.2}$$

$$\mathcal{Y}_t = h_\Theta\left(y_t\right) \tag{B.3}$$

$$\varepsilon_t \sim \mathcal{N}\left(0, \Sigma_\varepsilon\right) \tag{B.4}$$

The first equation determines the deterministic evolution of the endogenous variables in the absence of shocks summarized in vector $\tilde{y}_t$ with initial conditions y_0 and terminal (asymptotic) state y for a given set of nonlinear equations $g_\Theta\left(\cdot\right)$. The second equation determines the path of endogenous variables y_t with economic surprise, ε_t is a vector of exogenous stochastic innovations that are normally distributed with mean zero and covariance Σ_ε; Θ is the vector of structural parameters; $h_\Theta\left(\cdot\right)$ and $g_\Theta\left(\cdot\right)$ are the set of nonlinear equations. $\mathbb{E}_{t,t+S}\left\{\cdot\right\}$

is the extended path-consistent expectation operator, which updates expectations over a specific time horizon of size S, and takes as given $\tilde{y}_{t+S+1}$ the terminal period of the expectation. Therefore, the size of the expectation window S must be sufficiently large to ensure that the value of $\tilde{y}_{t+S+1}$ does not affect the outcome.[34] The third equation relates the observations summarized in the vector $\mathcal{Y}_t$ to the endogenous variables in y_t. The last equation concerns the distribution of exogenous innovations.

For each evaluation of the sample likelihood, we first compute the deterministic path providing the transition between the initial period $\{\tilde{y}_t\}_{t=1}^{T}$ and the terminal period. We select a value of $T = 1,000$ to allow convergence to the terminal state. Formally, we use Equation B.1 assuming that (*i*) no shock with sequence $\{\varepsilon_t\}_{t=1}^{T}$ is all zeros, and (*ii*) a terminal condition that is the steady state of the model $\tilde{y}_{t+S+1} = y$, which can be written as $\tilde{y}_t = g_\Theta(y_{t_0}, y, 0)$. Next, we use the inversion filter to find the sequence of $\{\varepsilon_t\}_{t=1}^{T^*}$ that matches sample $\{\mathcal{Y}_t\}_{t=1}^{T^*}$ with T^* observations using $\{\tilde{y}_t\}_{t=1}^{T}$ as the terminal value of the expectation window. This implicitly assumes that agents expect the economy to return to its deterministic path $\tilde{y}$ after S periods. Based on the smoothed sequence $\{\varepsilon_t\}_{t=1}^{T^*}$, the likelihood function $\mathcal{L}(\theta, \mathcal{Y}_{1:T^*})$ of the model is obtained, conditional on the matrix of observations through time T^*.

Appendix C. Observable variables

Figure C.1. Observable variables



Appendix D. Model evaluation

The model's empirical performance is first evaluated by comparing observed and model-implied moments, as reported in Table D.1. Data moments are computed over the period 1985Q1-2023Q2, while model-implied moments are derived from 1,000 random draws from

[34] One must strike a balance between the length of the expectation window to mimic infinite-horizon rational expectations, and the computational burden of updating the expectations. We select an expectation horizon of 40 years ($S = 160$). This length is sufficiently large to ensure that the terminal conditions do not quantitatively affect the numerical value of the likelihood function, but exhibits a moderate computational burden.

the estimated posterior distributions of the model parameters. The table also includes 90% confidence intervals for the model-implied statistics. As shown in Table D.1, the model replicates key features of the data reasonably well, despite its relatively small scale.

TABLE D.1. Empirical and model-implied moments

	DATA	MODEL [5%;95%]	DATA	MODEL [5%;95%]
	Mean		**Standard deviations**	
Output growth	0.007	[0.007;0.008]	0.012	[0.014;.0.019]
Inflation rate	0.011	[0.000;0.015]	0.007	[0.004;0.010]
Nominal interest rate	0.008	[-0.000;0.015]	0.006	[0.004;0.010]
Carbon emission growth	0.004	[0.003;0.004]	0.013	[0.015;0.020]
	Autocorrelation		**Correlation w/ output**	
Output growth	-0.199	[-0.294;-0.013]	1.000	[1.000;1.000]
Inflation rate	0.977	[0.815;0.968]	0.204	[-0.177;0.234]
Nominal interest rate	0.988	[0.969;0.996]	-0.038	[-0.175;0.236]
Carbon emission growth	-0.100	[-0.281;0.007]	0.965	[0.877;0.945]

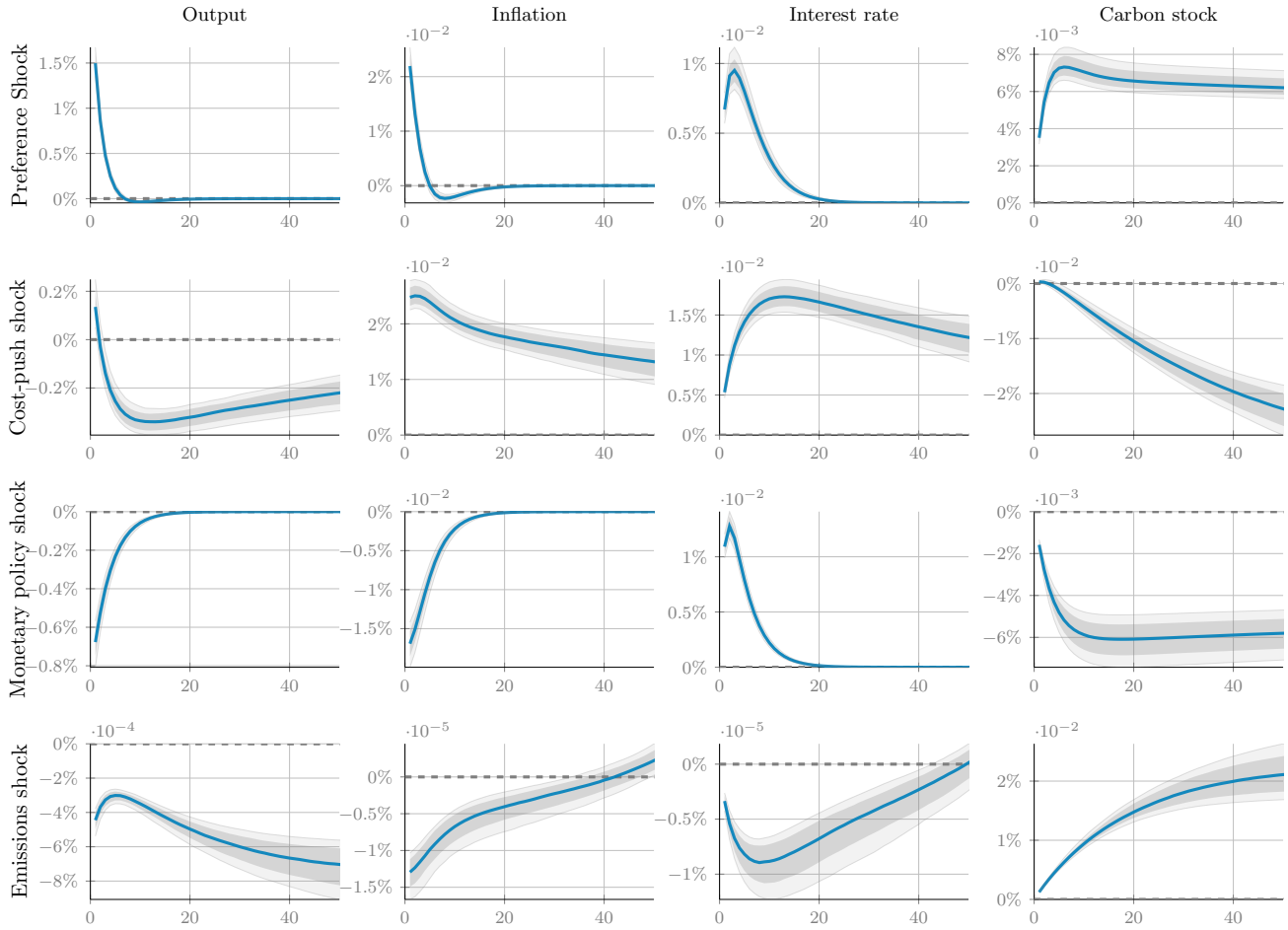
Note: Model-implied moments are computed across 1,000 random artificial series, each of the same size as the data sample.

Indeed, the model's performance is relatively strong when evaluated against typical benchmarks in the estimation of real business cycle models. In particular, it replicates relatively well the observed volatility of inflation and nominal interest rates with notable accuracy. However, the model tends to underestimate the volatility of output and carbon emissions, indicating potential areas for refinement. First-order autocorrelations are generally well matched, although the persistence of inflation is somewhat understated relative to the data. In terms of cross-correlations with output, the model captures the key relationships for most variables, and remain for carbon emission growth.

As a second step, model performance is assessed using impulse response functions (IRFs), which provide insight into the dynamic propagation of shocks through the economic and climate systems. Figure D.1 presents the generalized impulse responses of the estimated model, based on parameters evaluated at their posterior mode from the Metropolis-Hastings sampling.

The first row of Figure D.1 presents the responses to a positive preference shock that raises household consumption. In response, aggregate output increases, reflecting the stimulative effect of heightened perceived wealth on economic activity. This boost in output, in turn, leads to a rise in both inflation and the cumulative carbon stock. To counteract the inflationary pressure from this demand-driven expansion, the central bank raises the nominal interest

FIGURE D.1. Generalized impulse response functions of the estimated model



Note: The figure displays the generalized impulse response functions (GIRFs) of several variables for four shocks: preference, cost-push, monetary policy, and emissions in lines 1 to 4, respectively. The GIRFs are computed using the value of the state variables in 2023Q2, and each GIRF is expressed as a percentage deviation from its initial value in 2023. GIRFs are averaged based on 500 exogenous draws.

rate. As the shock dissipates over time, the tightening of monetary policy eventually induces a mild recession.

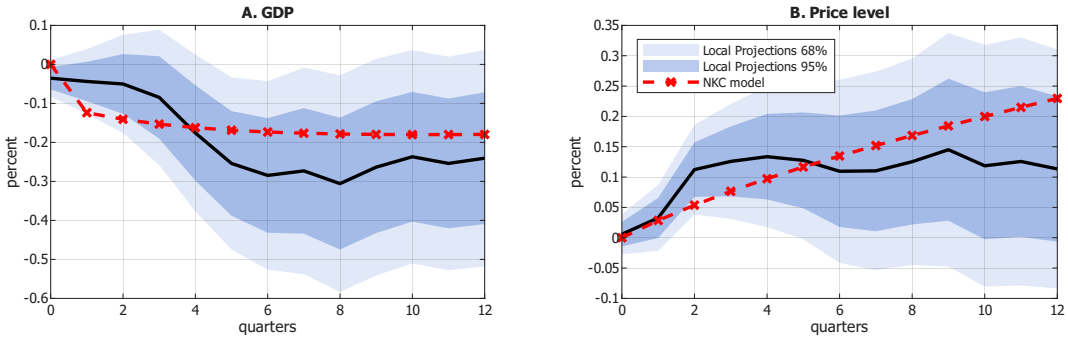
The second row of Figure D.1 reports the responses to a cost-push shock, similar to the markup shock in Smets and Wouters (2007). This adverse supply shock raises firms' pricing power and selling prices, exerting downward pressure on the rest of the economy. The central bank faces a classic trade-off between stabilizing prices and output, as the interest rate cannot simultaneously address movements in opposite directions. Following the shock, the real interest rate rises modestly, leading to a delayed contraction in output. Interestingly, the drop in economic activity has a beneficial environmental side effect: reduced emissions due to lower production and demand.

The third row of Figure D.1 illustrates the impact of a monetary policy shock, modeled as a temporary deviation of the nominal interest rate from the systematic component of the policy rule. This shock increases the return on safe assets, discouraging consumption and compressing aggregate demand. Firms respond by cutting labor demand, which reduces equilibrium wages and marginal costs. Consequently, both output and prices decline, leading to a reduction in emissions and a lower-than-expected carbon stock.

The fourth row shows the effects of an emission intensity shock, interpreted as an exogenous increase in emissions per unit of output. This shock raises the carbon stock in the atmosphere and imposes moderate economic damage. However, its effects on inflation and nominal interest rates are negligible, suggesting that such shocks may have limited short-run macroeconomic implications.

A third exercise assesses the model's ability to replicate empirical evidence on the effects of a carbon price shock. Figure D.2 contrasts the impulse responses of GDP and the price level to such a shock, as generated by our estimated New Keynesian Climate model, with those obtained from local projections on the same quarterly sample as Känzig (2023). In line with Bilal and Känzig (2024), this comparison connects theoretical predictions with reduced-form evidence. However, our approach differs in a key respect: instead of calibrating the model to match the impulse response functions, we estimate it using Bayesian methods on the full sample and subsequently validate it externally against the local projections. Despite these differences in identification and estimation, both approaches deliver qualitatively similar dynamics: a carbon price shock reduces GDP and an raises the price level.

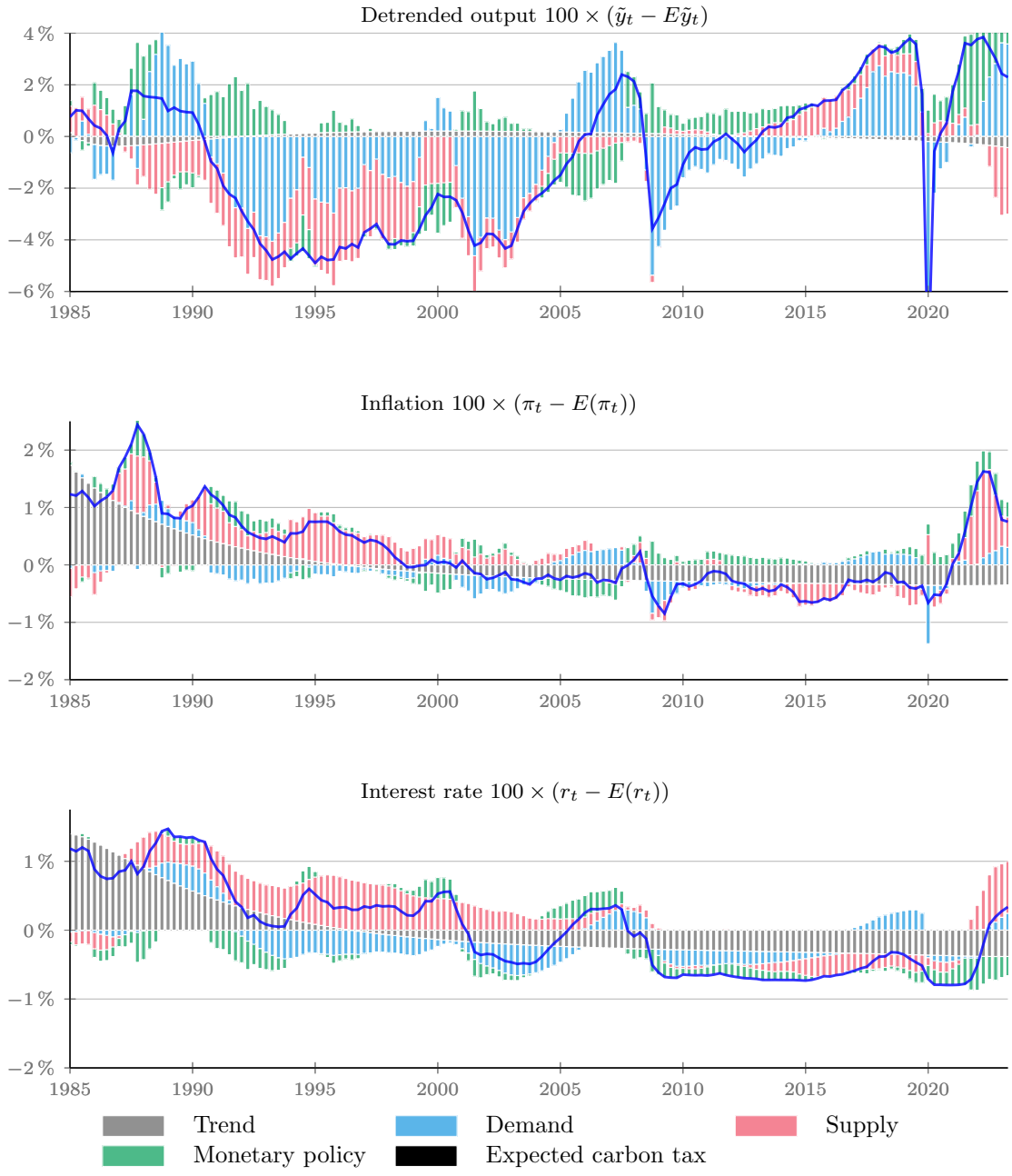
FIGURE D.2. Impulse responses to a carbon price shock



Note: This figure shows the responses of GDP (Panel A) and the price level (Panel B) to the carbon price shock identified by Känzig (2023). Shaded areas represent the 68% and 95% confidence bands from local projections, while the solid red line depicts the response from the estimated NKC model. For comparability, the structural model's inflation response is scaled so that its initial impact matches that observed in the local projections. Controls include 3 lags of the outcome variable and a linear trend.

Finally, Figure D.3 presents a historical decomposition of output, inflation, and the nominal interest rate, attributing their fluctuations to the identified structural shocks within the New Keynesian climate model. This decomposition offers a dynamic interpretation of the drivers behind key macroeconomic variables over time.

FIGURE D.3. Historical decomposition of detrended output, inflation and the nominal interest rate over the sample period



Note: This figure illustrates the approximate contribution of each structural shock to the determination of the variable of interest. Cross-products between shock contributions are omitted in the decomposition.

APPENDIX E. DETAILS ON THE DECOMPOSITION OF OUTPUT AND INFLATION

This appendix provides additional details on the decomposition of output and inflation.

E.1. **Demand part.** Detrended Euler equation reads as:

$$\tilde{\lambda}_t = \mathbb{E}_t \left\{ \beta \frac{r_t}{\pi_{t+1}} \left((1-\omega)\tilde{\lambda}_{t+1} + \omega \varepsilon_{b,t+1} \tilde{d}_{t+1}^{-\sigma_c} \right) \right\}.$$

It can be rewritten as:

$$\begin{aligned} \tilde{\lambda}_t &= \mathbb{E}_t \left\{ R_t \left((1-\omega)\tilde{\lambda}_{t+1} + \omega \varepsilon_{b,t+1} \tilde{d}_{t+1}^{-\sigma_c} \right) \right\} \\ &= \omega \mathbb{E}_t \left\{ \sum_{s=0}^{\infty} (1-\omega)^s \varepsilon_{b,t+s} \tilde{d}_{t+s}^{-\sigma_c} \prod_{j=0}^{s} R_{t+j} \right\}, \end{aligned}$$

where $R_t = \beta r_t / \mathbb{E}_t \{\pi_{t+1}\}$.

Recall that: $\tilde{\lambda}_t = \varepsilon_{b,t} \left(\frac{c_t/z_t - \omega \tilde{d}_t}{1-\omega} \right)^{-\sigma_c}$, the Euler equation becomes:

$$\left(\frac{c_t/z_t - \omega \tilde{d}_t}{(1-\omega)} \right)^{-\sigma_c} = \omega \mathbb{E}_t \left\{ \sum_{s=0}^{\infty} (1-\omega)^s \varepsilon_{b,t+s} \tilde{d}_{t+s}^{-\sigma_c} \prod_{j=0}^{s} R_{t+j} \right\}.$$

By denoting $IS_t = c_t/z_t$, we obtain:

$$IS_t = \omega \tilde{d}_t + (1-\omega) \left[\omega \mathbb{E}_t \left\{ \sum_{s=0}^{\infty} \beta (1-\omega)^s \varepsilon_{b,t+s} \tilde{d}_{t+s}^{-\sigma_c} \prod_{j=0}^{s} \frac{r_{t+j}}{\pi_{t+1+j}} \right\} \right]^{-1/\sigma_c}.$$

In addition, we know that $c_t/z_t = x_t y_t/(z_t l_t)$, where $x_t = 1 - \frac{\kappa}{2}(\pi_t - \pi_t^\star)^2 - \theta_{1,t} \tilde{\tau}_{e,t}^{\theta_2/(\theta_2-1)}$ and $\mu_t = \tilde{\tau}_{e,t}^{1/(\theta_2-1)}$.

Consequently,

$$IS_t = x_t \tilde{y}_t.$$

Finally, applying the logarithm yields:

$$\hat{y}_t \simeq \widehat{IS}_t + \theta_{1,t} \tilde{\tau}_{e,t}^{\theta_2/(\theta_2-1)} + \frac{\kappa}{2}(\pi_t - \pi_t^\star)^2,$$

with $\hat{y}_t = \log(\tilde{y}_t/\tilde{y})$ and $\widehat{IS}_t = \log(IS_t/IS)$.

E.2. **Supply part.** The dynamics of the inflation gap $\hat{\pi}_t = \pi_t - \pi_t^\star$ comes from the Phillips curve:

$$(\hat{\pi}_t + \pi_t^\star)\hat{\pi}_t = \sum_{s=0}^{+\infty} \frac{B_{t+s}^{\pi}(\tilde{y}_{t+s}, m_{t+s})}{B_t^{\pi}(\tilde{y}_t, m_t)} \left(\frac{1-\zeta}{\kappa} + \frac{\zeta}{\kappa} mc_{t+s}(\varepsilon_{t+s}^p, \tilde{y}_{t+s}, m_{t+s}, \tilde{\tau}_{e,t+s}) \right),$$

where $B_t^{\pi}(\cdot)$ and the marginal cost $mc_t(\cdot)$ are functions of four forces, namely, the cost-push shock (ε_t^p), detrended GDP ($\tilde{y}_t$), cumulative carbon emissions (m_t), and the carbon tax ($\tilde{\tau}_{e,t}$).

We use Shapley values to provide a rigorous and consistent decomposition of inflation dynamics across these interacting forces. Because the model is nonlinear, the effect of each force on inflation depends on which other forces are active. For instance, the inflationary impact of the carbon tax may differ depending on the state of output or cumulative emissions. This interdependence makes it impossible to attribute inflation changes uniquely through standard linear decomposition methods. The Shapley decomposition solves this problem by treating each force as a "player" in a cooperative game. It evaluates the marginal contribution of each force across all possible combinations (or "coalitions") of active forces and then computes the average contribution across these combinations. This ensures that each force receives a fair and order-invariant share of the total change in inflation, accounting for nonlinear interactions. Disabling a force means fixing it at its initial value in 2024Q1, i.e., $\{1,\ \tilde{y}_{2024Q1},\ m_{2024Q1}, \tilde{\tau}_{e,2024Q1}\}$, so that it remains constant along the counterfactual path. Note that the shock is normalized to 1 and neutralized to isolate its effect. In practical terms, the Shapley value for each force represents the average incremental impact of activating that force on the simulated inflation path, given all possible configurations of the other forces. As such, it provides a consistent measure of attribution, allowing us to disentangle the respective roles of demand, policy, and climate channels in driving inflation during the green transition.

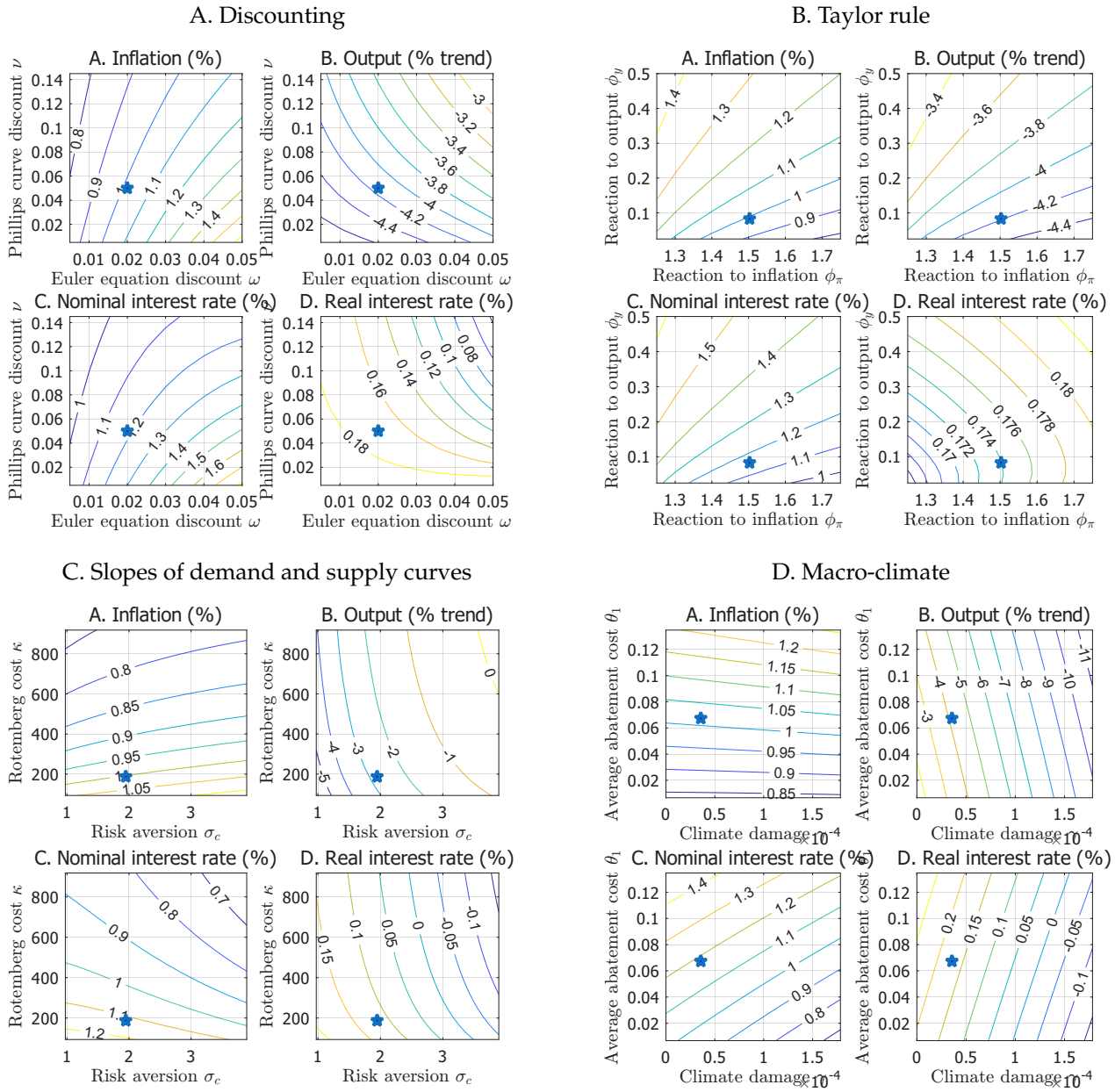
Appendix F. Sensitivity analysis

This appendix presents a sensitivity analysis exploring the impact of various structural parameters on inflation and output dynamics during the green transition.

F.1. **The role of attenuated expectations.** The forward guidance puzzle in New Keynesian models underscores a well-known issue: these models often predict unrealistically large effects of future policy announcements on current economic outcomes, leading to implausibly strong responses in output and inflation. A similar dynamic arises with an announced carbon tax, which induces disproportionately large anticipatory adjustments in current consumption and investment, driven by expectations of future policy impacts. To address this concern, we examine the sensitivity of our model to this puzzle. Our framework incorporates two key parameters, one in the Euler equation and another in the Phillips curve, that moderate the influence of forward-looking real interest rates and marginal costs on present economic dynamics. Panel A of Figure F.1 illustrates the average levels of inflation, output, nominal interest rate, and real interest rate under varying degrees of attenuation. Stronger attenuation,

implemented through more intense discounting of future marginal utilities of consumption, tends to increase inflation. By assigning less weight to future real interest rates, households front-load consumption during the transition, creating upward pressure on prices through the demand channel.

FIGURE F.1. Sensitivity to structural parameters



Note: This figure presents the average values of inflation, output, nominal interest rate, and real interest rate over the period from 2023Q4 to 2050Q1 under the Paris Agreement scenario. The star marker indicates the outcome based on the estimated parameter values.

Conversely, increased discounting also weakens the responsiveness of inflation to anticipated future marginal costs, such as those induced by a rising carbon tax, by flattening the

Phillips curve. This dampens inflationary pressures, and as a result, the economy experiences higher average output during the transition period due to more stable price dynamics.

F.2. **The Taylor rule.** An additional question concerns whether the monetary policy stance, characterized as either dovish or hawkish, influences macroeconomic dynamics during the transition period. To assess this, we vary the coefficients of the Taylor rule, focusing on a relatively high responsiveness to inflation $\phi_\pi \in [1.15, 2]$ and output $\phi_y \in [0.1, 1]$. Panel B of Figure F.1 presents the resulting outcome. Our findings are consistent with standard monetary stabilization mechanisms: increasing the inflation (respectively, output gap) coefficient tends to reduce average inflation (respectively, detrended output) during the transition. However, these effects are modest. A higher policy response coefficient does not lead to a proportionally large decline in the average value of the corresponding target variable. This result implies that the typical output-inflation trade-off, as discussed in Clarida et al. (1999) and Woodford (2003), is relatively weak in the context of the green transition. Furthermore, our analysis reveals that the divine coincidence, the principle whereby stabilizing inflation inherently stabilizes the output gap, does not hold. Specifically, increasing the weight on the output gap in the Taylor rule does not lead to a reduction in inflation. This suggests that the transition exhibits features of a supply-side shock, wherein attempts to stabilize real activity may be less effective in simultaneously managing price stability.

F.3. **Slopes of aggregate demand and supply curves.** Recent literature, including Hazell et al. (2022), has documented the relative flatness of the New Keynesian Phillips Curve (NKPC) since the 1980s. However, the recent surge in inflation, particularly following the economic disruptions caused by the war in Ukraine, has prompted a substantial reassessment of the price-setting mechanism. This reassessment has resulted in a significantly steeper NKPC, as shown in studies such as Harding et al. (2023) and Benigno and Eggertsson (2023). In light of these developments, we examine the sensitivity of our results to changes in the slope of the Phillips curve by varying the Rotemberg adjustment cost parameter from 50 to 120. In parallel, we also investigate the impact of the risk aversion coefficient in the household utility function. Within the New Keynesian framework, higher risk aversion reduces the responsiveness of households to real interest rate fluctuations, thereby weakening the monetary policy transmission channel. To this end, we explore values starting from 1.4, as used in Smets and Wouters (2007) and Nordhaus (2017), up to levels more commonly employed in the asset pricing literature. Panel C of Figure F.1 presents the outcomes of these sensitivity

exercises. We find that increasing the degree of nominal rigidity does reduce the responsiveness of inflation during the transition; however, the effect is quantitatively limited and does not materially alter the qualitative behavior of the model. This indicates that inflation dynamics during the transition are not highly sensitive to the specific calibration of nominal rigidities. By contrast, the risk aversion parameter plays a more critical role in shaping macroeconomic outcomes. A higher degree of risk aversion amplifies households' preference for consumption smoothing, reducing their sensitivity to real interest rate changes. As a result, aggregate consumption becomes less reactive to monetary policy shocks. This mechanism is especially important in determining output dynamics during the transition: when output is less sensitive to the real interest rate, contractionary effects from monetary tightening are mitigated. Under such conditions, abatement expenditures can become the dominant force, potentially allowing for an expansionary path even in the presence of carbon pricing and structural transformation.

F.4. **Macro-climate parameters.** We also examine the sensitivity of key macroeconomic variables to changes in macro-climate parameters. Specifically, Panel D of Figure F.1 presents the outcomes associated with varying the climate damage parameter (γ) and the abatement cost parameter (θ_1). To interpret γ, consider that in the baseline scenario with no mitigation policy, a carbon stock of 1,700 gigatons results in a total factor productivity loss of approximately 6.83%. We explore a range of values for γ, from zero climate damages to three times the calibrated baseline level (approximately 1.1×10^{-4}). For the abatement cost parameter θ_1, this can be interpreted as the average share of GDP required to achieve net-zero emissions. In our benchmark scenario, this cost is about 6.5% of GDP; we extend the analysis up to 13% of GDP to reflect more challenging decarbonization pathways. Our results indicate that inflation increases with both higher climate damages and higher abatement costs. This pattern is consistent with the earlier discussion of greenflation and climateflation. The imposition of carbon pricing policies, coupled with climate-induced disruptions to productivity, exerts upward pressure on production costs, thereby fueling inflation. Among the two parameters, abatement costs play a relatively larger role in shaping the cost of the transition. Higher abatement costs increase firms' marginal production costs, intensifying inflationary pressures through the greenflation channel. Similarly, a higher damage parameter raises inflation through the climateflation mechanism, while also exerting a contractionary effect on output. As damages grow, productivity deteriorates and real interest rates rise, which in turn reduces investment and consumption. Thus, the damage parameter emerges as a key driver of output dynamics during the transition period.